

Quantum critical phenomena of excitonic insulating transition in two dimensions

Xiao-Yin Pan,¹ Jing-Rong Wang,² and Guo-Zhu Liu^{3,*}

¹*Department of Physics, Ningbo University, Ningbo, Zhejiang 315211, China*

²*Anhui Province Key Laboratory of Condensed Matter Physics at Extreme Conditions,*

High Magnetic Field Laboratory of the Chinese Academy of Sciences, Hefei, Anhui 230031, China

³*Department of Modern Physics, University of Science and Technology of China, Hefei, Anhui 230026, China*

We study the quantum criticality of the phase transition between Dirac semimetal and excitonic insulator in two dimensions. Even though the system has a semimetallic ground state, there are observable effects of excitonic pairing at finite temperatures and/or finite energies, provided that the system is in proximity to excitonic insulating transition. To determine the quantum critical behavior, we consider three potentially important interactions, including the Yukawa coupling between Dirac fermion and excitonic order parameter fluctuation, the long-range Coulomb interaction, and the disorder scattering. We employ the renormalization group technique to study how these interactions separately affect quantum critical behavior and how they influence each other. We first investigate the Yukawa coupling in the clean limit, and show that it gives rise to typical non-Fermi liquid behavior. Adding random scalar potential to the system always turns such a non-Fermi liquid into a compressible diffusive metal. In comparison, the non-Fermi liquid behavior is further enhanced by random vector potential, but is nearly unaffected by random mass. Incorporating the Coulomb interaction changes these results qualitatively. In particular, the non-Fermi liquid state is protected by the Coulomb interaction for weak random scalar potential, and it becomes a diffusive metal only when random scalar potential becomes sufficiently strong. The interplay of Yukawa coupling, Coulomb interaction, and random vector potential (or random mass) induces a stable non-Fermi liquid state in which the fermion velocities take constant values in the lowest energy limit. These unusual quantum critical phenomena can be probed by measuring observable quantities. We also find that, while the fermion velocity anisotropy is not altered by the quantum fluctuation of excitonic order parameter, it is driven by the Coulomb interaction to flow to the isotropic limit.

I. INTRODUCTION

In the past decade, the unconventional properties of various Dirac/Weyl semimetal (SM) materials¹⁻⁹ have been investigated extensively. Many of the unconventional properties are related to the existence of isolated Dirac/Weyl points, at which the conduction and valence bands touch. When the chemical potential is tuned to exactly the Dirac points, the fermion density of states (DOS) vanishes at the Fermi level. As a result, the Coulomb interaction is long-ranged due to the absence of static screening. Extensive previous studies^{1,10-33} have revealed that the Coulomb interaction leads to a variety of unconventional low-energy behaviors.

Among all the known SM materials, two-dimensional Dirac SM, abbreviated as 2D DSM hereafter, has been studied most extensively, usually in the context of graphene¹. Renormalization group (RG) analysis^{1,34} revealed that the long-range Coulomb interaction is marginally irrelevant in the weak-coupling regime. When the Coulomb interaction is strong enough, the originally massless fermions can acquire a dynamical mass gap via the formation of stable particle-hole pairs³⁵⁻⁷⁴. This gap generating scenario is non-perturbative, and has the same picture as excitonic pairing, a notion proposed decades ago^{75,76}. In the special case of 2D DSM, such an excitonic gap dynamically breaks a continuous chiral (sublattice) symmetry, which can be regarded as a condensed-matter realization of the dynamical chiral symmetry breaking^{77,78}. The finite gap opened at the

Dirac point drives the SM to undergo a quantum phase transition (QPT) into an excitonic insulator (EI). The EI is induced only when the effective interaction strength, denoted by α , exceeds a critical value α_c , which defines SM-EI quantum critical point (QCP).

In recent years, the possibility of SM-EI transition in graphene has been studied by carrying out theoretical and numerical calculations. Early calculations^{35-41,60-62} predicted that the Coulomb interaction in suspended graphene is strong enough to open an excitonic gap at zero temperature. Specifically, the critical value α_c was found to be smaller than the physical value $\alpha = 2.16$ (in vacuum). However, no visible experimental evidence for excitonic gap has been observed at low temperatures⁷⁹. More careful calculations^{47,50,51,67-69} discovered that the critical value is actually $\alpha_c > 2.16$, which precludes the existence of excitonic gap in zero-temperature suspended graphene. Owing to the conceptual importance and also the potential technical applications, theorists are still searching for possible approaches to promote excitonic pairing in various SM materials. For instance, it was proposed that excitonic pairing may be promoted by an additional short-range repulsive interaction^{39,41,47} or by some extrinsic effects, such as strain⁸⁰.

Most previous works on SM-EI QPT have focused on the precise calculation of α_c at zero temperature ($T = 0$) by means of various techniques³⁵⁻⁷⁴. In this paper, we propose to explore the signatures of excitonic pairing at finite T and/or finite energy ω . Here is our logic: even though the exact zero- T ground state of suspended graphene (or other 2D DSMs) is gapless, the quantum

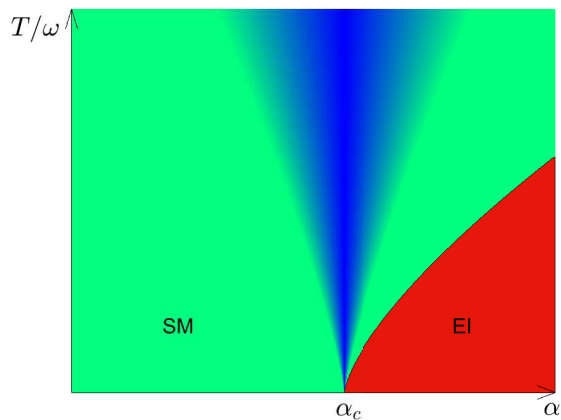


FIG. 1: Global phase diagram of 2D DSM on the α - T or α - ω plane. Here, ω stands for the fermion energy. Deep in the insulating phase, the fermions are suppressed at low energies. Deep in the semimetallic phase, the Coulomb interaction is too weak to form excitonic pairs. The excitonic insulating transition occurs as α increases up to α_c at $T = 0$. This point is broadened into a finite quantum critical regime at finite T and/or finite ω . The excitonic quantum fluctuation has observable effects in the whole quantum critical regime.

fluctuation of excitonic pairs still have observable effects at finite T and/or ω if the system is located in the quantum critical regime around the putative SM-EI QCP. Indeed, recent Monte Carlo simulations⁶⁷ and Dyson-Schwinger equation study⁵⁴ suggest that the value α_c is close to the physical value. The picture is illustrated in the schematic global phase diagram shown in Fig. 1. If α is slightly smaller than α_c , no excitonic gap is opened at $T = 0$, and the excitonic order parameter has a vanishing mean-value. However, the quantum fluctuation of excitonic order parameter is not negligible at finite T/ω and may lead to considerable corrections to some observable quantities. For instance, after performing nuclear-magnetic-resonance measurements, Hirata *et al.*⁸¹ argued that α -(BEDT-TTF)₂I₃ is close to an SM-EI QCP and that the excitonic fluctuation results in singular corrections to the nuclear magnetic resonance relaxation rate⁸¹.

We will study the quantum critical phenomena emerging in the broad quantum critical regime around SM-EI QCP, with the aim to search for observable effects of excitonic pairing. For this purpose, we take suspended graphene (2D DSM) as a prototypical model, and analyze the interaction corrections to observable quantities of massless Dirac fermions. In this regime, the fermions are subject to the quantum fluctuation of excitonic order parameter, which is described by a Yukawa coupling term. The long-range Coulomb interaction is certainly present and needs to be taken into account. Moreover, there is always certain amount of quenched disorder in realistic materials, and the fermion-disorder coupling might play a crucial role at low T . The accurate quantum critical phenomena cannot be determined if one or more of these interactions are naively ignored or improperly treated.

Indeed, these three kinds of interaction can affect, either enhancing or suppressing, each other. To make a general analysis, we will consider all the three kinds of interaction, and study their impact on the quantum criticality as well as their mutual influence by means of RG approach.

As the first step, we treat the Yukawa coupling in the clean limit, and demonstrate that this coupling induces strong violation of Fermi liquid (FL) theory. Specifically, the quasiparticle residue Z_f vanishes at low energies, and the fermion DOS receive power-law corrections from Yukawa coupling, which are both typical non-Fermi-liquid (NFL) behaviors. If the fermion dispersion is originally anisotropic, the velocity ratio is unrenormalized.

The next step is to incorporate quenched disorder and analyze its interplay with the Yukawa coupling. We find that the resultant low-energy properties depend sensitively on the nature of the disorder. Adding random scalar potential (RSP) to the system always turns the NFL caused by Yukawa coupling in the clean limit into a compressible diffusive metal (CDM). The CDM is characterized by the generation of a finite zero-energy fermion DOS and a constant zero- T disorder scattering rate. Different from RSP, random vector potential (RVP) tends to further enhance the NFL behavior, whereas random mass (RM) has negligible effects on the system.

We finally incorporate the Coulomb interaction, and find that it changes the above results qualitatively. In the case of weak RSP, the Coulomb interaction suppresses disorder scattering and as such renders the stability of the NFL state caused by Yukawa coupling. However, this NFL state is converted into CDM state once RSP becomes sufficiently strong. The combination of Yukawa coupling, Coulomb interaction, and RVP gives rise to a stable NFL state in which the fermion velocities flow to constant values in the lowest energy limit. If the Yukawa coupling, Coulomb interaction, and RM are considered simultaneously, we show that the Coulomb interaction is marginally irrelevant and RM is irrelevant. All of these quantum critical phenomena can be experimentally detected by measuring observable quantities.

Our results might be applied to understand some 2D DSM materials, such as uniaxially strained graphene^{52,53} and organic compound α -(BEDT-TTF)₂I₃⁸¹. In these systems, the fermion velocities along different directions may be unequal. It is therefore necessary to examine how interactions change the velocity anisotropy. According to our RG analysis, the fermion velocity anisotropy is unaffected by the quantum fluctuation of excitonic order parameter, but the system is driven by the Coulomb interaction to flow to the isotropic limit.

The rest of the paper will be arranged as following. The model is presented in Sec. II. The RG equations for the corresponding parameters are shown in Sec. III. The numerical results for different conditions are given and analyzed in Sec. IV. The main results are summarized in Sec. V. The detailed derivation of the RG equations can be found in Appendices.

II. THE MODEL

The fermion energy dispersion in intrinsic graphene is isotropic. It becomes anisotropic when graphene is deformed. Generically, the action of free 2D Dirac fermions with anisotropic dispersion is given by

$$S_f = \sum_{\sigma=1}^N \int_{\tau, \mathbf{x}} \bar{\Psi}_{\sigma}(\tau, \mathbf{x}) [\partial_{\tau} \gamma_0 + \mathcal{H}_f] \Psi_{\sigma}(\tau, \mathbf{x}), \quad (1)$$

where $\int_{\tau, \mathbf{x}} \equiv \int d\tau \int d^2\mathbf{x}$ and $\mathcal{H}_f = -iv_1 \nabla_1 \gamma_1 - iv_2 \nabla_2 \gamma_2$. Here, Ψ is two component spinor, and $\bar{\Psi} = \Psi^{\dagger} \gamma_0$. The 4×4 matrices $\gamma_{0,1,2}$ are defined as $\gamma_{0,1,2} = (\tau_3, -i\tau_2, i\tau_1) \otimes \tau_3$ in terms of Pauli matrices τ_i with $i = 1, 2, 3$. The gamma matrices satisfy the anti-commutative rule $\{\gamma_{\mu}, \gamma_{\nu}\} = 2\text{diag}(1, -1, -1)$. The fermion species is denoted by σ , which sums from 1 to N . Fermion flavor N is assumed to be a general large integer. v_1 and v_2 are the fermion velocities along two orthogonal directions.

The action of excitonic order parameter can be written as

$$S_b = \int_{\tau, \mathbf{x}} \left[\frac{1}{2} (\partial_{\tau} \phi)^2 + \frac{c^2}{2} (\nabla \phi)^2 + \frac{r}{2} \phi^2 + \frac{u}{24} \phi^4 \right], \quad (2)$$

where c is the boson velocity. Varying boson mass r tunes the QPT between SM and EI phases. At the QCP, the mass vanishes, i.e., $r = 0$, and the massless bosonic field ϕ represents the quantum critical fluctuation of excitonic order parameter. The quartic self-coupling is measured by parameter u . The Yukawa coupling between fermions and excitonic order parameter is given by

$$S_b = \lambda \sum_{\sigma=1}^N \int_{\tau, \mathbf{x}} \phi \bar{\Psi}_{\sigma} \Psi_{\sigma}, \quad (3)$$

where λ is the coupling constant.

The excitonic pairing originates from the Coulomb interaction between fermions and their anti-fermions (holes). Inside the EI phase, a finite gap is opened at the Fermi level and strongly suppresses the low-energy fermion DOS. In this case, the Coulomb interaction and even the fermionic degrees of freedom can be neglected, and the low-energy properties of the EI phase is mainly governed by the dynamics of neutral excitons. In contrast, the fermions remain gapless at the SM-EI QCP. The Coulomb interaction between gapless fermions may play an important role at low energies. The action for Coulomb interaction is described by

$$S_{ee} = \frac{1}{4\pi} \sum_{\sigma, \sigma'=1}^N \int_{\tau, \mathbf{x}, \mathbf{x}'} \rho_{\sigma}(\tau, \mathbf{x}) \frac{e^2/\epsilon}{|\mathbf{x} - \mathbf{x}'|} \rho_{\sigma'}(\tau, \mathbf{x}'), \quad (4)$$

where $\int_{\tau, \mathbf{x}, \mathbf{x}'} \equiv \int d\tau \int d^2\mathbf{x} \int d^2\mathbf{x}'$. The fermion density operator is defined as $\rho_{\sigma}(\tau, \mathbf{x}) = \bar{\Psi}_{\sigma}(\tau, \mathbf{x}) \gamma_0 \Psi_{\sigma}(\tau, \mathbf{x})$. In addition, e is the electric charge and ϵ the dielectric constant.

Disorder exists universally in any realistic material. Many of the low-energy behaviors of gapless fermions are heavily affected by the disorder scattering, especially at low T . The fermion-disorder coupling is formally described by the action

$$S_{dis} = v_{\Gamma} \int d\tau d^2\mathbf{x} \bar{\Psi}_{\sigma}(\mathbf{x}) \Gamma \Psi_{\sigma}(\mathbf{x}) A(\mathbf{x}). \quad (5)$$

The random field $A(\mathbf{x})$ is assumed to be a Gaussian white noise, i.e., $\langle A(\mathbf{x}) \rangle = 0$ and $\langle A(\mathbf{x}) A(\mathbf{x}') \rangle = \Delta \delta^2(\mathbf{x} - \mathbf{x}')$. Here, Δ is the impurity concentration, whereas v_{Γ} measures the strength of a single impurity. The disorders are classified by the expression of Γ matrix. For $\Gamma_0 = \gamma_0$, $A(\mathbf{x})$ is a RSP. For $\Gamma_j = \mathbb{1}_4$, $A(\mathbf{x})$ serves as a RM. For $\Gamma = (\gamma_1, \gamma_2)$ and $v_{\Gamma} = (v_{\Gamma 1}, v_{\Gamma 2})$, $A_{1,2}(\mathbf{x})$ correspond to the two components of RVP.

The free fermion propagator has the form

$$G_0(\omega, \mathbf{k}) = \frac{1}{-i\omega \gamma_0 + v_1 k_1 \gamma_1 + v_1 k_2 \gamma_2}. \quad (6)$$

The Yukawa coupling can be treated by the RG method in combination with the $1/N$ expansion. Following the scheme developed by Huh and Sachdev⁸³, we rescale ϕ and r as follows: $\phi \rightarrow \phi/\lambda$ and $r \rightarrow Nr\lambda^2$. Accordingly, the bare propagator of ϕ is expressed as

$$D_0^A(\Omega, \mathbf{q}) = \frac{1}{\frac{\Omega^2 + c^2 \mathbf{q}^2}{\lambda^2} + Nr}. \quad (7)$$

Near the QCP, we take $r = 0$ and then get

$$D_0^A(\Omega, \mathbf{q}) = \frac{\lambda^2}{\Omega^2 + c^2 \mathbf{q}^2}. \quad (8)$$

The free boson propagator is drastically altered by the polarization function, which, to the leading order of $1/N$ expansion, is

$$\begin{aligned} \Pi^A(\Omega, \mathbf{q}) &= N \int \frac{d^2\mathbf{k}}{(2\pi)^2} \int \frac{d\omega}{2\pi} \text{Tr} [G_0(\mathbf{k}, \omega) \\ &\quad \times G_0(\mathbf{k} + \mathbf{q}, \omega + \Omega)] \\ &= \frac{N}{4v_1 v_2} \sqrt{\Omega^2 + v_1^2 q_1^2 + v_2^2 q_2^2}. \end{aligned} \quad (9)$$

Now the dressed boson propagator becomes

$$D^A(\Omega, \mathbf{q}) = \frac{1}{\frac{\Omega^2 + c^2 \mathbf{q}^2}{\lambda^2} + \Pi^A(\Omega, \mathbf{q})}. \quad (10)$$

It is obvious that Π^A dominates over the free term in the low-energy regime. Thus, the above expression can be further simplified to

$$D^A(\Omega, \mathbf{q}) \approx \frac{1}{\Pi^A(\Omega, \mathbf{q})}. \quad (11)$$

The bare Coulomb interaction is described by

$$D_0^B(\mathbf{q}) = \frac{2\pi e^2}{\epsilon |\mathbf{q}|}. \quad (12)$$

The dynamical screening is encoded in the polarization $\Pi^B(\mathbf{q})$, whose leading order expression is given by

$$\begin{aligned} \Pi^B(\Omega, \mathbf{q}) &= -N \int \frac{d^2\mathbf{k}}{(2\pi)^2} \int \frac{d\omega}{2\pi} \text{Tr} [\gamma_0 G_0(\mathbf{k}, \omega) \gamma_0 \\ &\quad \times G_0(\mathbf{k} + \mathbf{q}, \omega + \Omega)] \\ &= \frac{N}{8v_1 v_2} \frac{v_1^2 q_1^2 + v_2^2 q_2^2}{\sqrt{\Omega^2 + v_1^2 q_1^2 + v_2^2 q_2^2}}. \end{aligned} \quad (13)$$

The dressed Coulomb interaction can be written as

$$D^B(\Omega, \mathbf{q}) = \frac{1}{(D_0^B(\mathbf{q}))^{-1} + \Pi^B(\Omega, \mathbf{q})}. \quad (14)$$

In previous works on the quantum criticality of SM-EI transition, the interplay of Yukawa coupling, Coulomb interaction, and disorder has never been systematically studied. Here, we emphasize that all these three interactions could be very important at low energies and sometime may have substantial mutual influence on each other. Therefore, they should be treated equally.

III. COUPLED RENORMALIZATION GROUP EQUATIONS

The interplay of distinct interactions can be treated by using the perturbative RG approach. The detailed RG calculations are presented in the Appendices. In this section, we only list the coupled RG equations of a number of model parameters and then analyze their low-energy properties. The effective model contains several parameters, including v_1 , v_2 , and v_Γ . These parameters are renormalized by interactions. To specify how the interactions alter the fermion dispersion anisotropy, we need to compute the running behavior of velocity ratio v_2/v_1 . Moreover, to judge whether the FL theory is applicable, we also compute the flow equation of the residue Z_f .

After incorporating three types of interaction in a self-consistent way, we find that the coupled RG equations for Z_f , v_1 , v_2 , and v_2/v_1 can be written as

$$\frac{dZ_f}{d\ell} = (C_0^A + C_0^B - C_g) Z_f, \quad (15)$$

$$\frac{dv_1}{d\ell} = (C_0^A + C_0^B - C_1^A - C_1^B - C_g) v_1, \quad (16)$$

$$\frac{dv_2}{d\ell} = (C_0^A + C_0^B - C_2^A - C_2^B - C_g) v_2, \quad (17)$$

$$\frac{d(v_2/v_1)}{d\ell} = (C_1^A - C_2^A + C_1^B - C_2^B) \frac{v_2}{v_1}. \quad (18)$$

The RG equation for the parameter v_Γ takes the form

$$\frac{dv_\Gamma}{d\ell} = 0 \quad (19)$$

for RSP. For the two components of RVP, the equations

for $v_{\Gamma 1}$ and $v_{\Gamma 2}$ are

$$\frac{dv_{\Gamma 1}}{d\ell} = (C_0^A + C_0^B - C_1^A - C_1^B - C_g) v_{\Gamma 1}, \quad (20)$$

$$\frac{dv_{\Gamma 2}}{d\ell} = (C_0^A + C_0^B - C_2^A - C_2^B - C_g) v_{\Gamma 2}. \quad (21)$$

For RM, we obtain

$$\begin{aligned} \frac{dv_\Gamma}{d\ell} &= (2C_0^A + C_1^A + C_2^A + 2C_0^B - C_1^B - C_2^B \\ &\quad - 2C_g) v_\Gamma. \end{aligned} \quad (22)$$

Here, we introduce a new parameter C_g to characterize the effective strength of disorder. For RSP and RM, it is

$$C_g = \frac{v_\Gamma^2 \Delta}{2\pi v_1 v_2}. \quad (23)$$

For RVP, it is defined as

$$C_g = \frac{(v_{\Gamma 1}^2 + v_{\Gamma 2}^2) \Delta}{2\pi v_1 v_2}. \quad (24)$$

The three coefficients C_0^A , C_1^A , and C_2^A appearing in the coupled RG equations are

$$\begin{aligned} C_0^A &= \frac{1}{8\pi^3} \int_{-\infty}^{+\infty} dx \int_0^{2\pi} d\theta \\ &\quad \times \frac{x^2 - \cos^2 \theta - (v_2/v_1)^2 \sin^2 \theta}{(x^2 + \cos^2 \theta + (v_2/v_1)^2 \sin^2 \theta)^2} \mathcal{G}^A(x, \theta) \end{aligned} \quad (25)$$

$$\begin{aligned} C_1^A &= \frac{1}{8\pi^3} \int_{-\infty}^{+\infty} dx \int_0^{2\pi} d\theta \\ &\quad \times \frac{-x^2 + \cos^2 \theta - (v_2/v_1)^2 \sin^2 \theta}{(x^2 + \cos^2 \theta + (v_2/v_1)^2 \sin^2 \theta)^2} \mathcal{G}^A(x, \theta) \end{aligned} \quad (26)$$

$$\begin{aligned} C_2^A &= \frac{1}{8\pi^3} \int_{-\infty}^{+\infty} dx \int_0^{2\pi} d\theta \\ &\quad \times \frac{-x^2 - \cos^2 \theta + (v_2/v_1)^2 \sin^2 \theta}{(x^2 + \cos^2 \theta + (v_2/v_1)^2 \sin^2 \theta)^2} \mathcal{G}^A(x, \theta) \end{aligned} \quad (27)$$

where

$$\mathcal{G}^A(x, \theta) = \frac{1}{\frac{N}{4v_2/v_1} \sqrt{x^2 + \cos^2 \theta + (v_2/v_1)^2 \sin^2 \theta}}. \quad (28)$$

The coefficients C_0^B , C_1^B , and C_2^B are

$$\begin{aligned} C_0^B &= \frac{1}{8\pi^3} \int_{-\infty}^{+\infty} dx \int_0^{2\pi} d\theta \\ &\quad \times \frac{-x^2 + \cos^2 \theta + (v_2/v_1)^2 \sin^2 \theta}{(x^2 + \cos^2 \theta + (v_2/v_1)^2 \sin^2 \theta)^2} \mathcal{G}^B(x, \theta) \end{aligned} \quad (29)$$

$$\begin{aligned} C_1^B &= \frac{1}{8\pi^3} \int_{-\infty}^{+\infty} dx \int_0^{2\pi} d\theta \\ &\quad \times \frac{-x^2 + \cos^2 \theta - (v_2/v_1)^2 \sin^2 \theta}{(x^2 + \cos^2 \theta + (v_2/v_1)^2 \sin^2 \theta)^2} \mathcal{G}^B(x, \theta) \end{aligned} \quad (30)$$

$$C_2^B = \frac{1}{8\pi^3} \int_{-\infty}^{+\infty} dx \int_0^{2\pi} d\theta \times \frac{-x^2 - \cos^2 \theta + (v_2/v_1)^2 \sin^2 \theta}{(x^2 + \cos^2 \theta + (v_2/v_1)^2 \sin^2 \theta)^2} \mathcal{G}^B(x, \theta) \quad (31)$$

with

$$\mathcal{G}^B(x, \theta) = \frac{1}{\frac{1}{2\pi\alpha_1} + \frac{N}{8v_2/v_1} \frac{\cos^2 \theta + (v_2/v_1)^2 \sin^2 \theta}{\sqrt{x^2 + \cos^2 \theta + (v_2/v_1)^2 \sin^2 \theta}}}. \quad (32)$$

The parameter

$$\alpha_1 = \frac{e^2}{\epsilon v_1} \quad (33)$$

is defined to measure the effective strength of Coulomb interaction. Charge e is not renormalized due to the absence of logarithmic term in the polarization Π^{B1} , and ϵ is fixed in a given sample. The value of α_1 is primarily controlled by the renormalization of velocity v_1 .

The coupled RG equations can be simplified. According to Eq. (19), we know that

$$v_\Gamma = v_{\Gamma 0} \quad (34)$$

is ℓ independent for RSP. Thus we re-write C_g as

$$C_g = \frac{v_\Gamma^2 \Delta}{2\pi v_1 v_2}. \quad (35)$$

The RG equation for C_g is given by

$$\frac{dC_g}{d\ell} = (-2C_0^A - 2C_0^B + C_1^A + C_1^B + C_2^A + C_2^B + 2C_g) C_g. \quad (36)$$

For RVP, from Eqs. (16), (17), (20), and (21), one gets

$$\frac{d(v_{\Gamma 1}/v_1)}{d\ell} = 0, \quad \frac{d(v_{\Gamma 2}/v_2)}{d\ell} = 0, \quad (37)$$

which indicate that

$$\frac{v_{\Gamma 1}}{v_1} = \frac{v_{\Gamma 10}}{v_{10}}, \quad \frac{v_{\Gamma 2}}{v_2} = \frac{v_{\Gamma 20}}{v_{20}}. \quad (38)$$

Accordingly, C_g now can be written as

$$C_g = \frac{\Delta}{2\pi} \left(\frac{v_{\Gamma 10}^2}{v_{10}^2} \frac{v_1}{v_2} + \frac{v_{\Gamma 20}^2}{v_{20}^2} \frac{v_2}{v_1} \right). \quad (39)$$

The corresponding RG equation is

$$\frac{dC_g}{d\ell} = \frac{(v_{\Gamma 1}^2 - v_{\Gamma 2}^2) \Delta}{2\pi v_1 v_2} (-C_1^A - C_1^B + C_2^A + C_2^B). \quad (40)$$

For RM, through Eqs. (16), (17), and (22), we obtain the RG equation for C_g

$$\frac{dC_g}{d\ell} = (2C_0^A + 3C_1^A + 3C_2^A + 2C_0^B - C_1^B - C_2^B - 2C_g) C_g. \quad (41)$$

for RM.

IV. QUANTUM CRITICAL PHENOMENA

In this section, we will solve the RG equations and then apply the solutions to analyze the quantum critical phenomena. We adopt the following steps: first, examine the low-energy behaviors induced solely by the quantum critical fluctuation of excitonic order parameter; second, introduce quenched disorder into the system and study its interplay with the Yukawa coupling; finally, investigate the impact of Coulomb interaction on the results.

A. Non-Fermi liquid behavior induced by excitonic fluctuation

If 2D DSM is far from SM-EI transition, the ground state is a robust SM. While the Coulomb interaction is long-ranged, it can only produce normal FL behavior^{1,10,11,15}. As the system approaches to the SM-EI QCP, the excitonic fluctuation becomes stronger and eventually invalidates the FL description at $T = 0$. Now we illustrate how FL theory breaks down at the QCP by analyzing the solutions of RG equations.

In the clean limit, the excitonic fluctuation leads to the following RG equations

$$\frac{dZ_f}{d\ell} = C_0^A Z_f, \quad (42)$$

$$\frac{dv_1}{d\ell} = (C_0^A - C_1^A) v_1, \quad (43)$$

$$\frac{dv_2}{d\ell} = (C_0^A - C_2^A) v_2, \quad (44)$$

$$\frac{d(v_2/v_1)}{d\ell} = (C_1^A - C_2^A) \frac{v_2}{v_1}. \quad (45)$$

These equations will be solved in the isotropic and anisotropic cases in order.

1. Isotropic limit

We first consider the isotropic limit, i.e., $v_1 = v_2 = v$. In this case, we have

$$C_0^A = C_1^A = C_2^A = -\frac{2}{3\pi^2 N} = -\eta^A. \quad (46)$$

Accordingly, the RG equations can be simplified to

$$\frac{dZ_f}{d\ell} = -\eta^A Z_f, \quad (47)$$

$$\frac{dv}{d\ell} = 0. \quad (48)$$

Obviously, the velocity remains a constant, i.e., $v = v_0$. This means that the fermion dispersion is not renormalized and the dynamical exponents is $z = 1$. The specific heat behaves as

$$C_v(T) \sim T^{d/z} \sim T^2. \quad (49)$$

The residue is given by

$$Z_f = Z_{f0} e^{-\eta^A \ell} = e^{-\eta^A \ell}, \quad (50)$$

which flows to zero quickly in the limit $l \rightarrow \infty$. Z_f is connected to the real part of retarded self-energy via the definition

$$Z_f = \frac{1}{\left|1 - \frac{\partial}{\partial \omega} \text{Re} \Sigma^R(\omega)\right|}. \quad (51)$$

Employing the transformation $\omega = \omega_0 e^{-\ell}$, where ω_0 is certain starting energy scale, we find that

$$\text{Re} \Sigma^R(\omega) \sim \omega^{1-\eta^A}. \quad (52)$$

Using the Kramers-Kronig relation, we can easily obtain the imaginary part

$$\text{Im} \Sigma^R(\omega) \sim \omega^{1-\eta^A}, \quad (53)$$

which exhibits typical NFL behavior. Moreover, the renormalized DOS depends on ω as follows

$$\rho(\omega) \sim \omega^{1+\eta^A}. \quad (54)$$

2. Anisotropic case

In the generic anisotropic case, namely $v_1 \neq v_2$, we integrate over variable x in Eqs. (25)-(27) and find

$$\begin{aligned} C_0^A &= -\frac{v_2/v_1}{3\pi^3 N} \int_0^{2\pi} d\theta \frac{1}{(\cos^2 \theta + (v_2/v_1)^2 \sin^2 \theta)} \\ &= -\frac{v_2/v_1}{3\pi^3 N} \frac{2\pi}{v_2/v_1} = -\eta^A, \end{aligned} \quad (55)$$

$$\begin{aligned} C_1^A &= \frac{v_2/v_1}{3\pi^3 N} \int_0^{2\pi} d\theta \frac{\cos^2 \theta - 3(v_2/v_1)^2 \sin^2 \theta}{(\cos^2 \theta + (v_2/v_1)^2 \sin^2 \theta)^2} \\ &= \frac{v_2/v_1}{3\pi^3 N} \left(-\frac{2\pi}{v_2/v_1} \right) = -\eta^A, \end{aligned} \quad (56)$$

$$\begin{aligned} C_2^A &= \frac{v_2/v_1}{3\pi^3 N} \int_0^{2\pi} d\theta \frac{-3 \cos^2 \theta + (v_2/v_1)^2 \sin^2 \theta}{(\cos^2 \theta + (v_2/v_1)^2 \sin^2 \theta)^2} \\ &= \frac{v_2/v_1}{3\pi^3 N} \left(-\frac{2\pi}{v_2/v_1} \right) = -\eta^A, \end{aligned} \quad (57)$$

which are exactly the same as the isotropic case. Accordingly, the RG equations for v_1 and v_2 are

$$\frac{dv_1}{d\ell} = \frac{dv_2}{d\ell} = 0, \quad (58)$$

which implies that

$$v_1 = v_{10}, \quad v_2 = v_{20}. \quad (59)$$

Thus, the fermion velocities are not renormalized, and the anisotropy is fixed. The low-energy properties of specific heat $C_v(T)$, residue Z_f , fermion damping rate $|\text{Im} \Sigma^R(\omega)|$, and DOS $\rho(\omega)$ are the same as those obtained in the isotropic case.

B. Excitonic fluctuation and disorder

We then add disorder and examine how it affects the above results. Now the coupled RG equations of Z_f , v_1 , v_2 , and v_2/v_1 are given by

$$\frac{dZ_f}{d\ell} = (C_0^A - C_g) Z_f = -(\eta^A + C_g) Z_f, \quad (60)$$

$$\frac{dv_1}{d\ell} = (C_0^A - C_1^A - C_g) v_1 = -C_g v_1, \quad (61)$$

$$\frac{dv_2}{d\ell} = (C_0^A - C_2^A - C_g) v_2 = -C_g v_2, \quad (62)$$

$$\frac{d(v_2/v_1)}{d\ell} = (C_1^A - C_2^A) \frac{v_2}{v_1} = 0. \quad (63)$$

For RSP, C_g satisfies

$$\frac{dC_g}{d\ell} = 2C_g^2, \quad (64)$$

whose solution is

$$C_g = \frac{C_{g0}}{1 - 2C_{g0}\ell}. \quad (65)$$

It is obvious that this C_g diverges as $l \rightarrow \ell_c$, where $\ell_c = 1/2C_{g0}$. Substituting Eq. (65) into Eqs. (60)-(62), we obtain

$$Z_f = e^{-\eta^A \ell} \sqrt{1 - 2C_{g0}\ell}, \quad (66)$$

$$v_1 = v_{10} \sqrt{1 - 2C_{g0}\ell}, \quad (67)$$

$$v_2 = v_{20} \sqrt{1 - 2C_{g0}\ell}. \quad (68)$$

We can see that, Z_f , v_1 , and v_2 all flow to zero at $l \rightarrow \ell_c$. Such singular behaviors are generally believed to indicate the instability of the system: RSP drives the system into a disorder-dominated compressible diffusive metal (CDM). The characteristic feature of CDM is that, the fermions acquire a finite disorder scattering rate

$$\gamma_{\text{imp}} = |\text{Im} \Sigma^R(0)|. \quad (69)$$

In the meantime, the zero-energy DOS $\rho(0)$ also becomes finite, being a function of γ_{imp} . According to the calculations given in Refs.^{49,84}, the specific heat displays a linear-in- T behavior, namely

$$C_v(T) \sim T. \quad (70)$$

Therefore, the NFL quantum critical state realized in the clean limit is turned into a CDM once RSP is added to the system, even when RSP is very weak. The fermion damping effect, low-energy DOS, and specific heat of CDM phase are all distinct from those of NFL phase.

For RVP, the RG equation for C_g is

$$\frac{dC_g}{d\ell} = \frac{(v_{\Gamma 1}^2 - v_{\Gamma 2}^2) \Delta}{2\pi v_1 v_2} (-C_1^A + C_2^A) = 0, \quad (71)$$

which implies that

$$C_g = C_{g0}. \quad (72)$$

Substituting Eq. (72) into Eqs. (60)-(62) yields

$$Z_f = e^{-(\eta^A + C_{g0})\ell}, \quad (73)$$

$$v_1 = v_{10}e^{-C_{g0}\ell}, \quad (74)$$

$$v_2 = v_{20}e^{-C_{g0}\ell}. \quad (75)$$

The real and imaginary parts of retarded fermion self-energy are

$$\text{Re}\Sigma^R(\omega) \sim \omega^{1-(\eta^A + C_{g0})}, \quad (76)$$

$$\text{Im}\Sigma^R(\omega) \sim \omega^{1-(\eta^A + C_{g0})}, \quad (77)$$

which are still NFL-like behaviors. Comparing to the clean limit, Z_f approaches to zero more quickly and the fermion damping is more drastic. The velocity v goes to zero quickly with growing ℓ , thus the fermion dispersion is substantially altered. In addition, the dynamical exponent z becomes $z = 1 + C_{g0}$. It is easy to find that, the specific heat is

$$C_v(T) \sim T^{d/z} \sim T^{2/(1+C_{g0})}, \quad (78)$$

and the low-energy DOS is

$$\rho(\omega) \sim \omega^{(1-C_{g0})/(1+C_{g0})+\eta^A}. \quad (79)$$

An apparent conclusion is that, both the DOS and specific heat are enhanced by RVP at low energies.

For RM, the RG equation for C_g becomes

$$\frac{dC_g}{d\ell} = -8\eta^A C_g - 2C_g^2. \quad (80)$$

Its solution is

$$C_g(\ell) = \frac{4\eta^A C_{g0}}{(C_{g0} + 4\eta^A) e^{8\eta^A \ell} - C_{g0}}, \quad (81)$$

which vanishes quickly in the limit $\ell \rightarrow \infty$. Substituting Eq. (81) into Eqs. (60)-(62), we get

$$Z_f = e^{-\eta^A \ell} \sqrt{\frac{4\eta^A}{(C_{g0} + 4\eta^A) - C_{g0}e^{-8\eta^A \ell}}}, \quad (82)$$

$$v_1 = v_{10} \sqrt{\frac{4\eta^A}{(C_{g0} + 4\eta^A) - C_{g0}e^{-8\eta^A \ell}}}, \quad (83)$$

$$v_2 = v_{20} \sqrt{\frac{4\eta^A}{(C_{g0} + 4\eta^A) - C_{g0}e^{-8\eta^A \ell}}}. \quad (84)$$

In the low-energy regime, the residue still behaves as $Z_f \sim e^{-\eta^A \ell}$. From the ℓ -dependence of Z_f , we obtain

$$\text{Re}\Sigma^R(\omega) \sim \omega^{1-\eta^A}, \quad (85)$$

$$\text{Im}\Sigma^R(\omega) \sim \omega^{1-\eta^A}, \quad (86)$$

which are the same as the clean case. As shown by Eqs. (83) and (84), v_1 and v_2 approach to finite values in

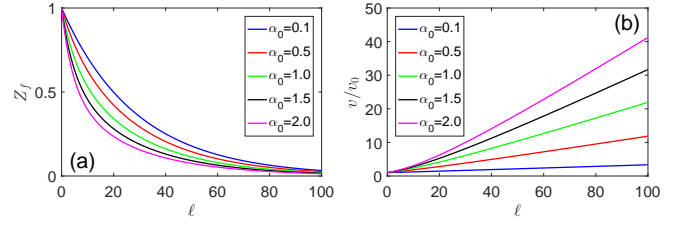


FIG. 2: Flowing behavior of Z_f and v caused by excitonic fluctuation and Coulomb interaction. In this and all the subsequent figures, we assume $N = 2$ in numerical calculations.

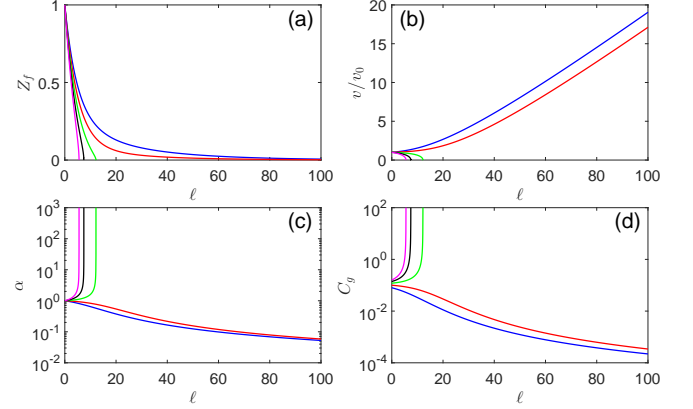


FIG. 3: Flowing behavior of Z_f , v , α , and C_g caused by excitonic fluctuation, Coulomb interaction, and RSP. Blue, red, green, black, and magenta lines correspond to $C_{g0} = 0.08, 0.1, 0.12, 0.14, 0.16$. Here, $\alpha_{10} = 1.0$.

the lowest energy limit. Accordingly, the fermion DOS still exhibits the behavior $\rho(\omega) \sim \omega^{1+\eta^A}$, and the specific heat is still of the form $C_v(T) \sim T^2$. We thus see that RM does not induce qualitative modifications to observable quantities at the SM-EI QCP.

From the above results, we infer that the low-energy properties of the SM-EI quantum critical system are dependent of the origin and features of the quenched disorder. These properties are embodied in such quantities as DOS and specific heat, which could be probed in experiments. However, we should remember that the Coulomb interaction is not taken into account in the above calculations. In the next subsection, we will study whether or not the above results are substantially affected when the Coulomb interaction is incorporated.

C. Interplay of three kinds of interaction

We now consider the interplay of excitonic quantum fluctuation (Yukawa coupling), Coulomb interaction, and disorder, first in the isotropic limit and then in the generic anisotropic case. We will see that the Coulomb interaction tends to suppress the fermion velocity anisotropy.

1. Isotropic limit

In the isotropic limit with $v_1 = v_2 = v$, the RG equations for Z_f and v are

$$\frac{dZ_f}{d\ell} = (-\eta^A + C_0^B - C_g) Z_f, \quad (87)$$

$$\frac{dv}{d\ell} = (C^B - C_g) v. \quad (88)$$

Here, $C^B = C_0^B - C_1^B = C_0 - C_2^B$, in which

$$C_0^B = \frac{4}{N\pi^2} \left[2 - \frac{1}{\lambda} \pi + \frac{2 - \lambda^2}{\lambda} f(\lambda) \right], \quad (89)$$

$$C_{1,2}^B = \frac{4}{N\pi^2} \left[1 - \frac{1}{\lambda} \frac{\pi}{2} + \frac{1 - \lambda^2}{\lambda} f(\lambda) \right]. \quad (90)$$

The variable λ is $\lambda = N\pi\alpha/4$, and the function $f(\lambda)$ is

$$f(\lambda) = \begin{cases} \frac{1}{\sqrt{1-\lambda^2}} \arccos(\lambda) & \lambda < 1 \\ \frac{1}{\sqrt{\lambda^2-1}} \operatorname{arccosh}(\lambda) & \lambda > 1 \\ 1 & \lambda = 1. \end{cases} \quad (91)$$

In the clean limit, Z_f and v flow according to

$$\frac{dZ_f}{d\ell} = (-\eta^A + C_0^B) Z_f, \quad (92)$$

$$\frac{dv}{d\ell} = C^B v. \quad (93)$$

The numerical solutions are shown in Fig. 2. The velocity v increases as the energy is lowered. The Coulomb interaction is marginally irrelevant since its strength parameter $\alpha = e^2/v\epsilon$ flows to zero slowly in the lowest energy limit. Both C_0^B and C^B vanish as $\alpha \rightarrow 0$. The velocity renormalization produces logarithmic-like correction to the temperature or energy dependence of some observable quantities, including specific heat and compressibility¹. The singular renormalization of fermion velocities has been observed by various experimental tools^{79,85-87}. At low energies, C_0^B is much smaller than η^A . Thus, the Coulomb interaction only slightly alters the low-energy behavior of Z_f induced by the excitonic fluctuation.

For RSP, the RG equation of C_g is

$$\frac{dC_g}{d\ell} = (-2C^B + 2C_g) C_g. \quad (94)$$

For a given α_0 , there exists a critical value $C^B(\alpha_0)$. The system exhibits entirely different low-energy properties when C_{g0} is greater and smaller than $C^B(\alpha_0)$. To illustrate this, we show the ℓ -dependence of Z_f , v , α , and C_g in Fig. 3. If $C_{g0} < C^B(\alpha_0)$, Z_f , α , and C_g all flow to zero as $\ell \rightarrow \infty$, but v increases with growing ℓ . These results indicate that weak RSP is suppressed by the Coulomb interaction. If $C_{g0} > C^B(\alpha_0)$, both C_g and

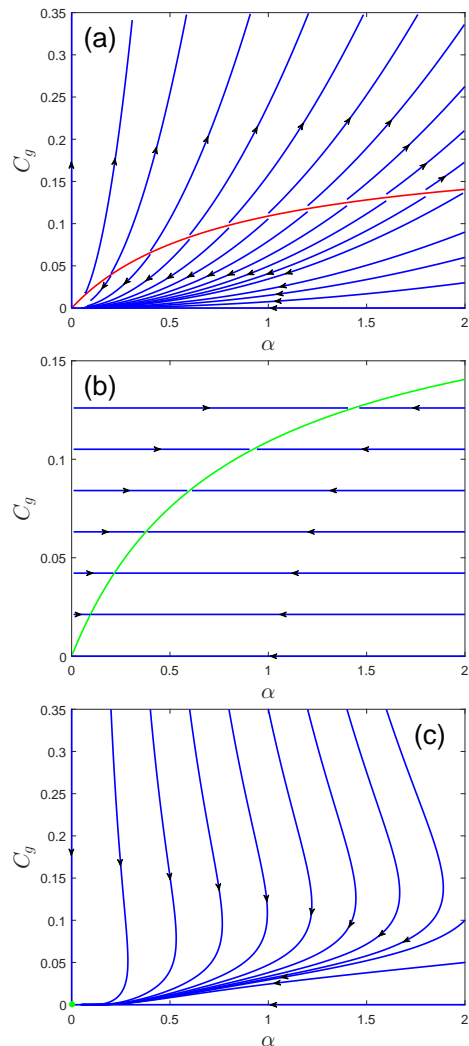


FIG. 4: Flowing diagrams on the α - C_g plane. Result for RSP is in (a), RGP in (b), and RM in (c).

α formally diverge at some finite energy scale, whereas both Z_f and v decrease rapidly down to zero at the same energy scale. Thus, strong RSP still drives a NFL-to-CDM transition. As can be seen from the flow diagram presented in Fig. 4(a), the (g_0, α_0) plane is divided by the critical line $C_{g0} = C^B(\alpha_0)$ into two distinct phases, namely the NFL phase and the CDM phase.

For RVP, the ℓ -dependence of Z_f , v , α , and C_g are presented in Fig. 5. Parameter C_g does not flow at all, namely

$$dC_g/d\ell = 0. \quad (95)$$

Thus we fix it at a constant, i.e., $C_g = C_{g0}$. For a given C_{g0} , v approaches to a constant value v^* in the zero energy limit. The value of v^* is obtained from

$$C^B(\alpha^*) = C_{g0}, \quad (96)$$

where $\alpha^* = e^2/v^*\epsilon$. RG analysis indicates that the system always flows to a stable infrared fixed point for any

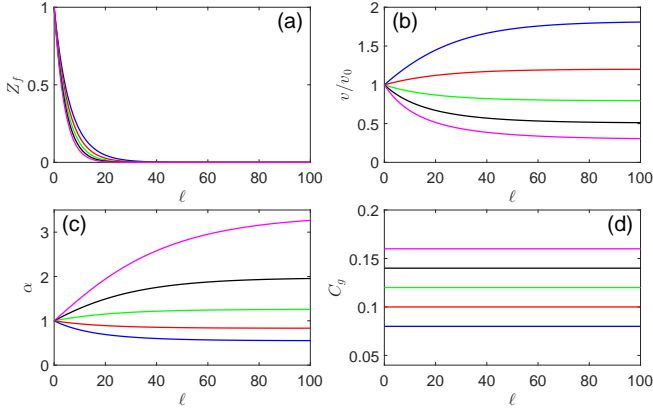


FIG. 5: Flowing behavior of Z_f , v , α , and C_g caused by excitonic fluctuation, Coulomb interaction, and RVP. Blue, red, green, black, and magenta lines correspond to $C_{g0} = 0.08, 0.1, 0.12, 0.14, 0.16$. Here, $\alpha_{10} = 1.0$.

two given initial values of α and C_g . Connecting all of these fixed points forms a critical line on the α - C_g plane, as shown in Fig. 4(b). Near the critical line, the specific heat behaves as

$$C_v(T) \sim \frac{1}{v^{*2}} T^2 \sim T^2. \quad (97)$$

The residue is

$$\begin{aligned} Z_f &\sim e^{(-\eta^A + C_0^B(\alpha^*) - C_{g0})\ell} \\ &\sim e^{(-\eta^A + C_1^B(\alpha^*))\ell}, \end{aligned} \quad (98)$$

where $C_1^B(\alpha^*)$ is negative. This Z_f flows to zero more quickly than the one induced purely by the excitonic fluctuation. The real and imaginary parts of retarded self-energy are

$$\text{Re}\Sigma^R(\omega) \sim \omega^{1-(\eta^A - C_1^B(\alpha^*))}, \quad (99)$$

$$\text{Im}\Sigma^R(\omega) \sim \omega^{1-(\eta^A - C_1^B(\alpha^*))}. \quad (100)$$

The DOS is found to behave as

$$\rho(\omega) \sim \omega^{1+\eta^A - C_1^B(\alpha^*)}. \quad (101)$$

For RM, the RG equation for C_g is given by

$$\frac{dC_g}{d\ell} = (-8\eta^A + 2C^B - 2C_g) C_g. \quad (102)$$

The numerical results are presented in Fig. 6. We observe that C_g always approaches to zero quickly, which represents that random mass is irrelevant in the low-energy regime. The Coulomb interaction is marginally irrelevant and leads to singular renormalization of fermion velocity. Accordingly, DOS and specific exhibits the behaviors:

$$\rho(\omega) \sim \frac{\omega^{1+\eta^A}}{\ln^2(\omega_0/\omega)}, \quad (103)$$

$$C_v(T) \sim \frac{T^2}{\ln^2(T_0/T)}. \quad (104)$$

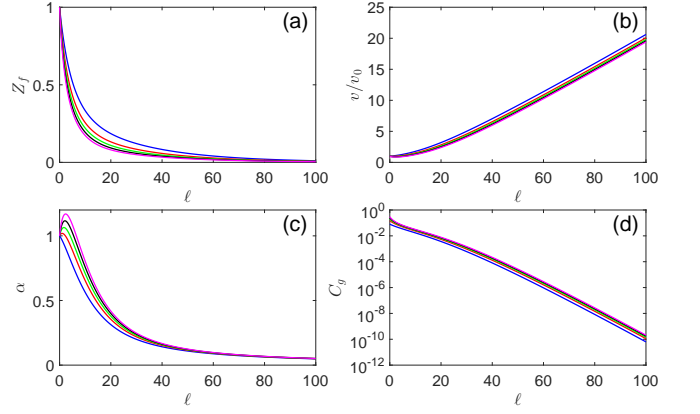


FIG. 6: Flowing behavior of Z_f , v , α , and C_g caused by excitonic fluctuation, Coulomb interaction, and RM. Blue, red, green, black, and magenta lines correspond to $C_{g0} = 0.08, 0.15, 0.2, 0.25, 0.3$. Here, $\alpha_{10} = 1.0$.

In the presence of RM, the two parameters (α, C_g) always flow to the stable infrared fixed point $(0, 0)$.

It is useful to compare the quantum critical phenomena to the low-energy behavior of the SM phase. Deep in the SM phase, the excitonic fluctuation can be completely ignored. The low-energy properties is primarily governed by the interplay of Coulomb interaction and disorder, which has already been extensively investigated^{49,88-93}. When Coulomb interaction and RSP are simultaneously present, the system is a normal FL if RSP is weak, but is turned into a CDM phase by strong RSP. Thus, increasing the effective strength of RSP drives a FL-to-CDM phase transition. In the SM-EI quantum critical regime, increasing the effective strength of RSP leads to a NFL-CDM transition. If RM is added to the system, it is irrelevant around the SM-EI QCP, but is marginal and results in a stable critical line on the α - C_g plane deep in the SM phase. In contrast, RVP produces the same qualitative low-energy behaviors in the SM phase and around the SM-EI QCP. To determine the true low-energy properties of the system, one could measure the fermion damping rate, DOS, and specific heat. Even in case 2D DSM has a gapless SM ground state, the fluctuation of excitonic order parameter still gives rise to observable effects at finite T/ω . The quantum critical regime can be distinguished from the pure SM phase by measuring the ω -dependence of fermion damping rate and/or the T -dependence of specific heat.

To provide a complete analysis of the quantum critical phenomena, we summarize in Table I the low-energy properties induced by all the possible combinations of three types of interaction. The quantities listed in Table I include the residue Z_f , damping rate $\text{Im}\Sigma^R(\omega)$, fermion DOS $\rho(\omega)$, and specific heat $C_v(T)$. An important indication is that, distinct interactions could affect each other significantly and thus need to be treated equally. The true quantum critical phenomena cannot be accurately determined if the interplay is not handled properly.

TABLE I: A summary of low-energy or low-temperature behaviors of some characteristic quantities caused by all the possible combination of the three types of interaction. Here, QFEO stands for the quantum fluctuation of excitonic order parameter. CI represents the Coulomb interaction. We choose to display the ℓ -dependent quasiparticle residue $Z_f(\ell)$, the zero-temperature fermion damping rate $\text{Im}\Sigma^R(\omega)$, the zero-temperature DOS $\rho(\omega)$, and the T -dependent $C_v(T)$. The definitions of all the notations are given in the main text.

Interaction	$Z_f(\ell)$	$\text{Im}\Sigma^R(\omega)$	$\rho(\omega)$	$C_v(T)$
QFEO	$e^{-\eta^A \ell}$	$\omega^{1-\eta^A}$	$\omega^{1+\eta^A}$	T^2
QFEO+RSP	$e^{-\eta^A \ell} \sqrt{1-2C_{g0}\ell}$	γ_{imp}	$\gamma_{\text{imp}} \ln(v\Lambda/\gamma_{\text{imp}})$	$\rho(0)T$
QFEO+RVP	$e^{-(\eta^A+C_{g0})\ell}$	$\omega^{1-(\eta^A+C_{g0})}$	$\omega^{(1-C_{g0})/(1+C_{g0})+\eta^A}$	$T^{2/(1+C_{g0})}$
QFEO+RM	$e^{-\eta^A \ell}$	$\omega^{1-\eta^A}$	$\omega^{1+\eta^A}$	T^2
QFEO+CI	$e^{-\eta^A \ell}$	$\omega^{1-\eta^A}$	$\omega^{1+\eta^A}/\ln^2(\omega_0/\omega)$	$T^2/\ln^2(T_0/T)$
QFEO+CI+RSP	$C_{g0} < C_B(\alpha_0)$	$e^{-\eta^A \ell}$	$\omega^{1+\eta^A}/\ln^2(\omega_0/\omega)$	$T^2/\ln^2(T_0/T)$
	$C_{g0} > C_B(\alpha_0)$	$\lim_{\ell \rightarrow l_c} Z_f(\ell) \rightarrow 0$	γ_{imp}	$\gamma_{\text{imp}} \ln(v\Lambda/\gamma_{\text{imp}})$
QFEO+CI+RVP	$e^{(-\eta^A+C_1^B(\alpha^*))\ell}$	$\omega^{1-(\eta^A-C_1^B(\alpha^*))}$	$\omega^{1+\eta^A-C_1^B(\alpha^*)}$	T^2
QFEO+CI+RM	$e^{-\eta^A \ell}$	$\omega^{1-\eta^A}$	$\omega^{1+\eta^A}/\ln^2(\omega_0/\omega)$	$T^2/\ln^2(T_0/T)$
CI	$\lim_{\ell \rightarrow \infty} Z_f(\ell) \rightarrow \text{Const.}$	$\omega/\ln^2(\omega_0/\omega)$	$\omega/\ln^2(\omega_0/\omega)$	$T^2/\ln^2(T_0/T)$
CI+RSP	$C_{g0} < C_B(\alpha_0)$	$\lim_{\ell \rightarrow \infty} Z_f(\ell) \rightarrow \text{Const.}$	$\omega/\ln^2(\omega_0/\omega)$	$\omega/\ln^2(\omega_0/\omega)$
	$C_{g0} > C_B(\alpha_0)$	$\lim_{\ell \rightarrow l_c} Z_f(\ell) \rightarrow 0$	γ_{imp}	$\gamma_{\text{imp}} \ln(v\Lambda/\gamma_{\text{imp}})$
CI+RVP	$e^{C_1^B(\alpha^*)\ell}$	$\omega^{1+C_1^B(\alpha^*)}$	$\omega^{1-C_1^B(\alpha^*)}$	T^2
CI+RM	$e^{C_1^B(\alpha^*)\ell}$	$\omega^{1+C_1^B(\alpha^*)}$	$\omega^{1-C_1^B(\alpha^*)}$	T^2

2. Anisotropic case

For different values of fermion velocity ratio, the running behaviors of Z_f , v_1 , v_2 , and v_2/v_1 obtained in the clean limit are plotted in Figs. 7(a)-(d), respectively. Firstly, Z_f flows to zero very quickly, implying the violation of FL description. This is essentially induced by the excitonic quantum fluctuation, because the Coulomb interaction by itself would yield a finite Z_f . Secondly, the two fermion velocities v_1 and v_2 both increase as the energy is lowered, whereas the velocity ratio v_2/v_1 flows to unity in the lowest energy limit. Remember that the excitonic quantum fluctuation does not renormalize fermion velocities at all, as illustrated in Sec. IV A. It is clear that the renormalization of v_1 and v_2 are mainly determined by the Coulomb interaction. These results indicate that both excitonic fluctuation and Coulomb interaction are important in the low-energy region.

After including three types of disorder, we find that the system still flows to the isotropic limit as the lowest energy is approached. The numerical results obtained in the cases of RSP, RVP, and RM are presented in Fig. 8, Fig. 9, and Fig. 10, respectively.

First, we consider the case of RSP. As shown in Fig. 8, for given values of α_{10} and C_{g0} , C_g becomes divergent at some finite energy scale if the bare velocity ratio v_{20}/v_{10} exceeds a critical value. Both Z_f and fermion velocities flow to zero at the same energy scale. The anisotropy is suppressed, but the ratio does not flow to the isotropic limit. If the bare value v_{20}/v_{10} is small, C_{g0} flows to zero quickly as the energy is lowered. Meanwhile, the fermion

velocities increase, and the ratio $v_2/v_1 \rightarrow 1$. Apparently, the isotropic limit is mainly driven by the Coulomb interaction. The residue Z_f still vanishes, owing to the excitonic fluctuation. For given values of α_{10} and C_{g0} , varying the velocity ratio v_{20}/v_{10} leads to QPT between CDM phase and NFL phase.

In case of RVP, we show the evolution of Z_f , v_1 , v_2/v_1 , and C_g in Fig. 9. Comparing to the clean limit, the velocity ratio v_2/v_1 approaches to unity more quickly. This should be attributed to the fact that the Coulomb interaction strength α flows to certain finite value in the presence of RVP but vanishes in the clean limit. Therefore, the suppression of anisotropy is more significant once RVP is introduced.

We finally turn to the impact of RM. According to Fig. 10, the disorder parameter C_g of RM always flows to zero quickly with decreasing energy. The low-energy behaviors of Z_f and v_1 are nearly the same as those obtained in the clean limit, and the velocity ratio $v_2/v_1 \rightarrow 1$ as the energy is lowered down to zero.

V. SUMMARY AND DISCUSSION

In summary, we have performed a systematic study of the quantum critical phenomena around the SM-EI transition point in the context of 2D DSM. The Yukawa coupling between Dirac fermions and excitonic quantum fluctuation, the Coulomb interaction, and the disorder scattering are treated on equal footing, focusing on their mutual influence and the consequent low-energy behavior of the quantum critical regime. We first studied the in-

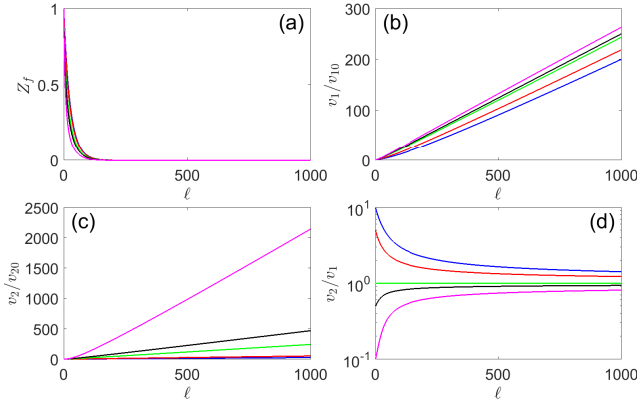


FIG. 7: Flowing behavior of Z_f , v_1 , v_2 , and v_2/v_1 caused by excitonic fluctuation and Coulomb interaction in the anisotropic case. Blue, red, green, black, and magenta lines correspond to $v_{20}/v_{10} = 10, 5, 1, 0.5, 0.1$. We choose $\alpha_{10} = 1.0$. As $\ell \rightarrow \infty$, the systems to the isotropic limit.

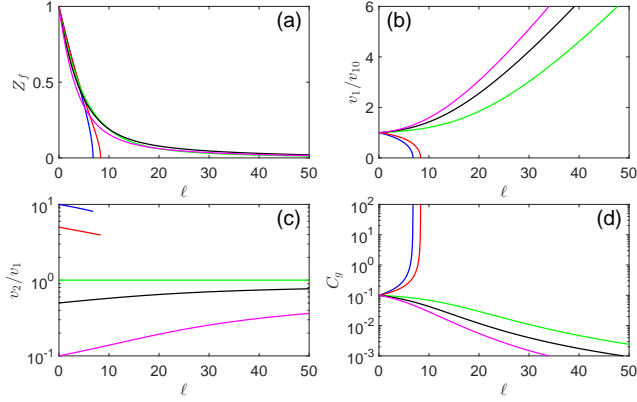


FIG. 8: Flowing behavior of Z_f , v_1 , v_2/v_1 , and C_g caused by excitonic fluctuation, Coulomb interaction, and RSP. Blue, red, green, black, and magenta lines correspond to $v_{20}/v_{10} = 10, 5, 1, 0.5, 0.1$. Here, $\alpha_{10} = 1.0$ and $C_{g0} = 0.1$.

fluence of quantum critical fluctuation of excitonic order parameter, and showed that it invalidates the FL description. We further demonstrated that, adding RSP always drives a NFL-to-CDM transition, and adding RVP further reinforces the NFL behaviors. Nevertheless, adding RM does not change the qualitative results obtained in the clean limit. Once Coulomb interaction is also incorporated, the above results are altered. In particular, the NFL state is protected by the Coulomb interaction for weak RSP, but is eventually replaced by CDM state if RSP is strong enough. When RVP or RM coexist with excitonic fluctuation and Coulomb interaction, the system is in a NFL state. To characterize the NFL and CDM phases, we have calculated several quantities, including the residue, damping rate, fermion DOS, and specific heat. The predicted quantum critical phenomena can be directly probed by experiments.

The results obtained in this paper might be applied to judge whether or not a 2D DSM is close to the SM-EI

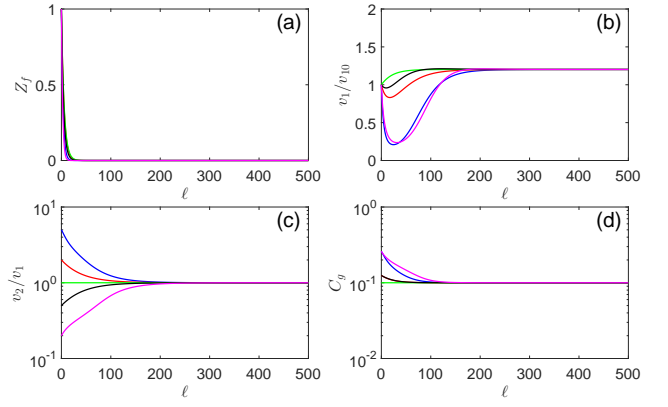


FIG. 9: Flowing behavior of Z_f , v_1 , v_2/v_1 , and C_g caused by excitonic fluctuation, Coulomb interaction, and RVP. Blue, red, green, black, and magenta lines correspond to $v_{20}/v_{10} = 5, 2, 1, 0.5, 0.2$. Here, $\alpha_{10} = 1.0$, $\Delta/2\pi = 0.05$, $v_{\Gamma 10}/v_{10} = 1$, and $v_{\Gamma 20}/v_{20} = 1$.

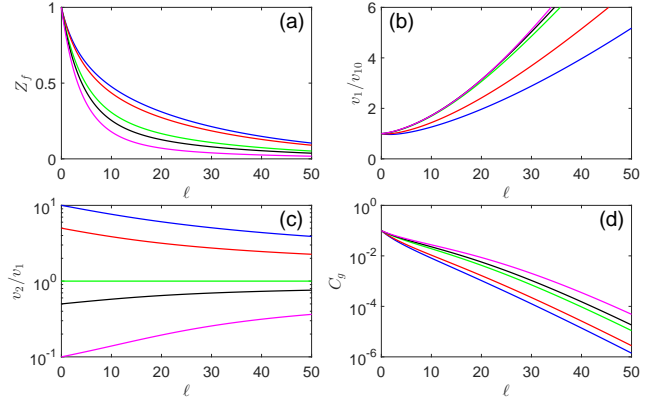


FIG. 10: Flowing behavior of Z_f , v_1 , v_2/v_1 , and C_g caused by excitonic fluctuation, Coulomb interaction, and RM. Blue, red, green, black, and magenta lines correspond to $v_{20}/v_{10} = 10, 5, 1, 0.5, 0.1$. $\alpha_{10} = 1.0$ and $C_{g0} = 0.1$.

QCP. Deep in the gapless SM phase, the properties of the system are governed by the combination of Coulomb interaction and disorder. As the system approaches the SM-EI QCP, i.e., $\alpha \rightarrow \alpha_c$, the excitonic quantum fluctuation becomes progressively more important, driving the system to enter into the quantum critical regime. Even if the zero- T ground state remains strictly gapless, the system exhibits nontrivial quantum critical behaviors in a number of observable quantities at finite temperatures and/or finite energies, as schematically illustrated in Fig. 1.

We thank Jing Wang and Peng-Lu Zhao for helpful discussions. We acknowledge the financial support by the National Natural Science Foundation of China under Grants 11275100, 11504379, and 11574285. X.Y.P. also acknowledges the support by the K.C. Wong Magna Foundation in Ningbo University. J.R.W. is partly supported by the Natural Science Foundation of Anhui Province under Grant 1608085MA19.

Appendix A: Polarization functions

We calculate the polarization functions contributed by particle-hole collective excitations. There are two different ways to define polarization function, corresponding to the dynamical screening effects of the quantum critical fluctuation of excitonic order parameter and the long-range Coulomb interaction, respectively.

1. Polarization function for excitonic fluctuation

For the quantum excitonic fluctuation, the polarization function is defined as

$$\begin{aligned} \Pi^A(\Omega, \mathbf{q}) &= N \int \frac{d\omega}{2\pi} \int \frac{d^2\mathbf{k}}{(2\pi)^2} \text{Tr} [G_0(\omega, \mathbf{k}) \\ &\quad \times G_0(\omega + \Omega, \mathbf{k} + \mathbf{q})]. \end{aligned} \quad (\text{A1})$$

Substituting the free fermion propagator into Eq. (A1), we obtain

$$\Pi^A(\Omega, \mathbf{q}) = -\frac{4N}{v_1 v_2} \int \frac{d^3k}{(2\pi)^3} \frac{k \cdot (k + q)}{k^2(k + q)^2}, \quad (\text{A2})$$

where $k = (\omega, \mathbf{k})$. Here, we have employed the following transformations

$$v_1 k_1 \rightarrow k_1, \quad v_2 k_2 \rightarrow k_2, \quad v_1 q_1 \rightarrow q_1, \quad v_2 q_2 \rightarrow q_2. \quad (\text{A3})$$

Using the Feynman parametrization formula

$$\frac{1}{AB} = \int_0^1 dx \frac{1}{[Ax + (1-x)B]^2}, \quad (\text{A4})$$

one gets

$$\begin{aligned} \Pi^A(\Omega, \mathbf{q}) &= -\frac{4N}{v_1 v_2} \int_0^1 dx \int \frac{d^3k}{(2\pi)^3} \\ &\quad \times \frac{k \cdot (k + q)}{[(k + xq)^2 + x(1-x)q^2]}. \end{aligned} \quad (\text{A5})$$

Let $k + xq \rightarrow k$, Π_A can be further written as

$$\begin{aligned} \Pi^A(\Omega, \mathbf{q}) &= -\frac{4N}{v_1 v_2} \int_0^1 dx \left\{ \int \frac{d^3k}{(2\pi)^3} \frac{k^2}{[k^2 + x(1-x)q^2]^2} \right. \\ &\quad \left. - \int \frac{d^3k}{(2\pi)^3} \frac{x(1-x)q^2}{[k^2 + x(1-x)q^2]^2} \right\}. \end{aligned} \quad (\text{A6})$$

Performing integration over k by using the standard formula of dimensional regularization

$$\int \frac{d^d k}{(2\pi)^d} \frac{1}{(k^2 + \Delta)^n} = \frac{1}{(4\pi)^{d/2}} \frac{\Gamma(n - \frac{d}{2})}{\Gamma(n)} \frac{1}{\Delta^{n - \frac{d}{2}}}, \quad (\text{A7})$$

$$\int \frac{d^d k}{(2\pi)^d} \frac{k^2}{(k^2 + \Delta)^n} = \frac{1}{(4\pi)^{d/2}} \frac{d}{2} \frac{\Gamma(n - \frac{d}{2} - 1)}{\Gamma(n)} \frac{1}{\Delta^{n - \frac{d}{2} - 1}}, \quad (\text{A8})$$

we find that

$$\begin{aligned} \Pi^A(\Omega, \mathbf{q}) &= \frac{2N}{v_1 v_2 \pi} \sqrt{q^2} \int_0^1 dx \sqrt{x(1-x)} \\ &= \frac{N}{4v_1 v_2} \sqrt{\Omega^2 + q_1^2 + q_2^2}. \end{aligned} \quad (\text{A9})$$

By taking $q_1 \rightarrow v_1 q_1$ and $q_2 \rightarrow v_2 q_2$, we get

$$\Pi^A(\Omega, \mathbf{q}) = \frac{N}{4v_1 v_2} \sqrt{\Omega^2 + v_1^2 q_1^2 + v_2^2 q_2^2}. \quad (\text{A10})$$

2. Polarization function for Coulomb interaction

For the Coulomb interaction, the polarization function is given by

$$\begin{aligned} \Pi^B(\Omega, \mathbf{q}) &= -N \int \frac{d\omega}{2\pi} \int \frac{d^2\mathbf{k}}{(2\pi)^2} \text{Tr} [\gamma_0 G_0(\omega, \mathbf{k}) \gamma_0 \\ &\quad \times G_0(\omega + \Omega, \mathbf{k} + \mathbf{q})]. \end{aligned} \quad (\text{A11})$$

Substituting Eq. (6) into Eq. (A11) leads to

$$\Pi^B(\Omega, \mathbf{q}) = \frac{4N}{v_1 v_2} \int \frac{d^3k}{(2\pi)^3} \frac{2k_0(k_0 + q_0) - k \cdot (k + q)}{k^2(k + q)^2}. \quad (\text{A12})$$

Making use of the Feynman parametrization formula Eq. (A4), along with the transformation $k + xq \rightarrow k$, we recast the above expression as

$$\begin{aligned} \Pi^B(\Omega, \mathbf{q}) &= \frac{4N}{v_1 v_2} \int_0^1 dx \left\{ \int \frac{d^3k}{(2\pi)^3} \frac{-k^2/3}{[k^2 + x(1-x)q^2]^2} \right. \\ &\quad \left. + \int \frac{d^3k}{(2\pi)^3} \frac{x(1-x)(q^2 - 2q_0^2)}{[k^2 + x(1-x)q^2]^2} \right\}. \end{aligned} \quad (\text{A13})$$

Repeating the calculational steps that lead to Eq.(A10), we finally obtain

$$\Pi^B(\Omega, \mathbf{q}) = \frac{N}{8v_1 v_2} \frac{v_1^2 q_1^2 + v_2^2 q_2^2}{\sqrt{\Omega^2 + v_1^2 q_1^2 + v_2^2 q_2^2}}. \quad (\text{A14})$$

Appendix B: Self-energy of fermion excitations

The fermion self-energy corrections come from three sorts of interaction, namely the Yukawa coupling, Coulomb interaction, and disorder scattering. The former two interactions are inelastic, and the third one is elastic. We now calculate them in order.

1. Contribution from Yukawa coupling

The fermion self-energy induced by the Yukawa coupling takes the form

$$\begin{aligned}\Sigma^A(\omega, \mathbf{k}) &= \int' \frac{d\Omega}{2\pi} \frac{d^2\mathbf{q}}{(2\pi)^2} G_0(\Omega + \omega, \mathbf{q} + \mathbf{k}) D^A(\Omega, \mathbf{q}) \\ &= - \int' \frac{d\Omega}{2\pi} \frac{d^2\mathbf{q}}{(2\pi)^2} \frac{[-i(\Omega + \omega)\gamma_0 + v_1(q_1 + k_1)\gamma_1 + v_2(q_2 + k_2)\gamma_2]}{[(\Omega + \omega)^2 + v_1^2(q_1 + k_1)^2 + v_2^2(q_2 + k_2)^2]} D^A(\Omega, \mathbf{q}).\end{aligned}\quad (\text{B1})$$

This self-energy can be expanded in powers of $i\omega$, v_1k_1 , and v_2k_2 . To the leading order, we get

$$\Sigma^A(\omega, \mathbf{k}) = i\omega\gamma_0 \int' \frac{d\Omega}{2\pi} \frac{d^2\mathbf{q}}{(2\pi)^2} \frac{-\Omega^2 + v_1^2q_1^2 + v_2^2q_2^2}{(\Omega^2 + v_1^2q_1^2 + v_2^2q_2^2)^2} \frac{1}{\frac{N}{4v_1v_2} \sqrt{\Omega^2 + v_1q_1^2 + v_2q_2^2}} \quad (\text{B2})$$

$$-v_1k_1\gamma_1 \int' \frac{d\Omega}{2\pi} \frac{d^2\mathbf{q}}{(2\pi)^2} \frac{\Omega^2 - v_1^2q_1^2 + v_2^2q_2^2}{(\Omega^2 + v_1^2q_1^2 + v_2^2q_2^2)^2} \frac{1}{\frac{N}{4v_1v_2} \sqrt{\Omega^2 + v_1q_1^2 + v_2q_2^2}} \quad (\text{B3})$$

$$-v_2k_2\gamma_2 \int' \frac{d\Omega}{2\pi} \frac{d^2\mathbf{q}}{(2\pi)^2} \frac{\Omega^2 + v_1^2q_1^2 - v_2^2q_2^2}{(\Omega^2 + v_1^2q_1^2 + v_2^2q_2^2)^2} \frac{1}{\frac{N}{4v_1v_2} \sqrt{\Omega^2 + v_1q_1^2 + v_2q_2^2}}. \quad (\text{B4})$$

To carry out RG calculation, we choose to integrate over the integral variables within the range

$$\int' \frac{d\Omega}{2\pi} \frac{d^2\mathbf{q}}{(2\pi)^2} = \frac{1}{8\pi^3} \int_{-\infty}^{+\infty} d\Omega \int_0^{2\pi} d\theta \int_{b\Lambda}^{\Lambda} d|\mathbf{q}|, \quad (\text{B5})$$

where $b = e^{-\ell}$. It is then easy to obtain

$$\Sigma^A(\omega, \mathbf{k}) = (-i\omega\gamma_0 C_0^A + v_1k_1\gamma_1 C_1^A + v_2k_2\gamma_2 C_2^A) \ell. \quad (\text{B6})$$

The expressions of C_i^A are given by Eqs. (25)-(28).

2. Contribution from Coulomb interaction

The fermion self-energy induced by the Coulomb interaction is

$$\begin{aligned}\Sigma^B(\omega, \mathbf{k}) &= - \int' \frac{d\Omega}{2\pi} \frac{d^2\mathbf{q}}{(2\pi)^2} \gamma_0 G(\Omega + \omega, \mathbf{q} + \mathbf{k}) \gamma_0 D^B(\Omega, \mathbf{q}) \\ &= \int' \frac{d\Omega}{2\pi} \frac{d^2\mathbf{q}}{(2\pi)^2} \gamma_0 \frac{[-i(\Omega + \omega)\gamma_0 + v_1(q_1 + k_1)\gamma_1 + v_2(q_2 + k_2)\gamma_2]}{[(\Omega + \omega)^2 + v_1^2(q_1 + k_1)^2 + v_2^2(q_2 + k_2)^2]} \gamma_0 D^B(\Omega, \mathbf{q}).\end{aligned}\quad (\text{B7})$$

To the leading order of small energy/momenta expansion, Σ_B can be approximately written as

$$\begin{aligned}\Sigma^B(\omega, \mathbf{k}) &= -i\omega\gamma_0 \int' \frac{d\Omega}{2\pi} \frac{d^2\mathbf{q}}{(2\pi)^2} \frac{-\Omega^2 + v_1^2q_1^2 + v_2^2q_2^2}{(\Omega^2 + v_1^2q_1^2 + v_2^2q_2^2)^2} \frac{1}{\frac{|\mathbf{q}|}{2\pi\epsilon^2} + \frac{N}{8v_1v_2} \frac{v_1^2q_1^2 + v_2^2q_2^2}{\sqrt{\Omega^2 + v_1^2q_1^2 + v_2^2q_2^2}}} \\ &\quad -v_1k_1\gamma_1 \int' \frac{d\Omega}{2\pi} \frac{d^2\mathbf{q}}{(2\pi)^2} \frac{\Omega^2 - v_1^2q_1^2 + v_2^2q_2^2}{(\Omega^2 + v_1^2q_1^2 + v_2^2q_2^2)^2} \frac{1}{\frac{|\mathbf{q}|}{2\pi\epsilon^2} + \frac{N}{8v_1v_2} \frac{v_1^2q_1^2 + v_2^2q_2^2}{\sqrt{\Omega^2 + v_1^2q_1^2 + v_2^2q_2^2}}} \\ &\quad -v_2k_2\gamma_2 \int' \frac{d\Omega}{2\pi} \frac{d^2\mathbf{q}}{(2\pi)^2} \frac{\Omega^2 + v_1^2q_1^2 - v_2^2q_2^2}{(\Omega^2 + v_1^2q_1^2 + v_2^2q_2^2)^2} \frac{1}{\frac{|\mathbf{q}|}{2\pi\epsilon^2} + \frac{N}{8v_1v_2} \frac{v_1^2q_1^2 + v_2^2q_2^2}{\sqrt{\Omega^2 + v_1^2q_1^2 + v_2^2q_2^2}}}.\end{aligned}\quad (\text{B8})$$

Performing integrations according to Eq. (B5), we obtain

$$\Sigma^B(\omega, \mathbf{k}) = (-i\omega\gamma_0 C_0^B + v_1 k_1 \gamma_1 C_1^B + v_2 k_2 \gamma_2 C_2^B) \ell. \quad (\text{B9})$$

The expressions of C_i^B can be found in Eqs. (29)-(32).

3. Contribution from disorder scattering

The fermion self-energy generated by disorder is

$$\begin{aligned} \Sigma_{dis}(\omega) &= \Delta v_\Gamma^2 \int' \frac{d^2 \mathbf{k}}{(2\pi)^2} \Gamma G_0(\mathbf{k}, \omega) \Gamma \\ &= i\omega v_\Gamma^2 \Delta \int' \frac{d^2 \mathbf{k}}{(2\pi)^2} \frac{\Gamma \gamma_0 \Gamma}{(\omega^2 + v_1^2 k_1^2 + v_2^2 k_2^2)} \\ &= i\omega \gamma_0 C_g \ell, \end{aligned} \quad (\text{B10})$$

where

$$C_g = \frac{v_\Gamma^2 \Delta}{2\pi v_1 v_2} \quad (\text{B11})$$

for both RSP and RM, and

$$C_g = \frac{(v_{\Gamma 1}^2 + v_{\Gamma 2}^2) \Delta}{2\pi v_1 v_2} \quad (\text{B12})$$

for RVP.

Appendix C: Corrections for the fermion-disorder coupling

The fermion-disorder coupling receive vertex corrections from three sorts of interaction, including the Yukawa coupling, the Coulomb interaction, and the fermion-disorder interaction, which will be studied in order.

1. Vertex correction from Yukawa coupling

The vertex correction induced by the Yukawa coupling is

$$V^A = - \int' \frac{d\Omega}{2\pi} \frac{d^2 \mathbf{q}}{(2\pi)^2} G_0(\Omega, \mathbf{q}) v_\Gamma \Gamma G_0(\Omega, \mathbf{q}) D^A(\Omega, \mathbf{q}). \quad (\text{C1})$$

For RSP, $\Gamma = \gamma_0$ and we get

$$V^A = v_\Gamma \gamma_0 (-C_0^A) \ell. \quad (\text{C2})$$

For the two components of RVP defined by $\Gamma = \gamma_1$ and $\Gamma = \gamma_2$, V_A is given by

$$V^A = v_\Gamma \gamma_1 (-C_1^A) \ell, \quad (\text{C3})$$

and

$$V^A = v_\Gamma \gamma_2 (-C_2^A) \ell, \quad (\text{C4})$$

respectively. For RM with $\Gamma = \mathbb{1}$, V_A is

$$V^A = v_\Gamma \mathbb{1} (C_0^A + C_1^A + C_2^A) \ell. \quad (\text{C5})$$

2. Vertex correction from Coulomb interaction

The vertex correction coming for the Coulomb interaction takes the form

$$\begin{aligned} V^B &= - \int' \frac{d\Omega}{2\pi} \frac{d^2 \mathbf{q}}{(2\pi)^2} \gamma_0 G_0(\Omega, \mathbf{q}) v_\Gamma \Gamma G_0(\Omega, \mathbf{q}) \gamma_0 \\ &\quad \times D^B(\Omega, \mathbf{q}). \end{aligned} \quad (\text{C6})$$

For RSP with $\Gamma = \gamma_0$, V_B is

$$V^B = v_\Gamma \gamma_0 (-C_0^B) \ell. \quad (\text{C7})$$

For the two components of RVP defined by $\Gamma = \gamma_1$ and $\Gamma = \gamma_2$, we obtain

$$V^B = v_\Gamma \gamma_1 (-C_1^B) \ln(b^{-1}), \quad (\text{C8})$$

and

$$V^B = v_\Gamma \gamma_2 (-C_2^B) \ln(b^{-1}), \quad (\text{C9})$$

respectively. For RM with $\Gamma = \mathbb{1}$, we find

$$V^B = v_\Gamma \mathbb{1} (C_0^B - C_1^B - C_2^B) \ell. \quad (\text{C10})$$

3. Vertex correction from disorder

The vertex correction due to fermion-disorder coupling has the form

$$\begin{aligned} V_{dis} &= \Delta v_\Gamma^2 \int' \frac{d^2 \mathbf{p}}{(2\pi)^2} \Gamma G_0(0, \mathbf{k}) v_\Gamma \Gamma G_0(0, \mathbf{k}) \Gamma \\ &= v_\Gamma \Delta v_\Gamma^2 \int' \frac{d^2 \mathbf{p}}{(2\pi)^2} \frac{1}{(v_1^2 k_1^2 + v_2^2 k_2^2)^2} \\ &\quad \times \Gamma (v_1 k_1 \gamma_1 + v_2 k_2 \gamma_2) \Gamma (v_1 k_1 \gamma_1 + v_2 k_2 \gamma_2) \Gamma. \end{aligned} \quad (\text{C11})$$

For RSP with $\gamma = \gamma_0$, V_{dis} is

$$V_{dis} = v_\Gamma \gamma_0 C_g \ell. \quad (\text{C12})$$

For the two components of RVP defined by $\gamma = \gamma_1$ and γ_2 , V_{dis} is

$$V_{dis} = 0. \quad (\text{C13})$$

For RM with $\Gamma = \mathbb{1}$, V_{dis} is

$$V_{dis} = -v_\Gamma \mathbb{1} C_g \ell. \quad (\text{C14})$$

Appendix D: Derivation of the RG equations

The action for the free fermions is given by

$$S_\Psi = \sum_{\sigma=1}^N \int \frac{d\omega}{2\pi} \frac{d^2\mathbf{k}}{(2\pi)^2} \bar{\Psi}_\sigma(\omega, \mathbf{k}) (-i\omega\gamma_0 + v_1 k_1 \gamma_1 + v_2 k_2 \gamma_2) \Psi_\sigma(\omega, \mathbf{k}). \quad (\text{D1})$$

Including the fermion self-energies induced by excitonic quantum fluctuation, long-range Coulomb interaction, and disorder scattering, the action of fermions becomes

$$\begin{aligned} S_\Psi &= \sum_{\sigma=1}^N \int \frac{d\omega}{2\pi} \frac{d^2\mathbf{k}}{(2\pi)^2} \bar{\Psi}_\sigma(\omega, \mathbf{k}) [-i\omega\gamma_0 + v_1 k_1 \gamma_1 + v_2 k_2 \gamma_2 - \Sigma^A(\omega, \mathbf{k}) - \Sigma^B(\omega, \mathbf{k}) - \Sigma_{dis}(\omega)] \Psi_\sigma(\omega, \mathbf{k}) \\ &\approx \sum_{\sigma=1}^N \int \frac{d\omega}{2\pi} \frac{d^2\mathbf{k}}{(2\pi)^2} \bar{\Psi}_\sigma(\omega, \mathbf{k}) \left[-i\omega\gamma_0 e^{-(C_0^A - C_0^B + C_g)\ell} + v_1 k_1 \gamma_1 e^{-(C_1^A + C_1^B)\ell} + v_2 k_2 \gamma_2 e^{-(C_2^B + C_2^B)\ell} \right] \Psi_\sigma(\omega, \mathbf{k}) \end{aligned} \quad (\text{D2})$$

Making the following re-scaling transformations:

$$\omega = \omega' e^{-\ell}, \quad (\text{D3})$$

$$k_1 = k'_1 e^{-\ell}, \quad (\text{D4})$$

$$k_2 = k'_2 e^{-\ell}, \quad (\text{D5})$$

$$\Psi = \Psi' e^{\left(2 + \frac{C_0^A}{2} + \frac{C_0^B}{2} - \frac{C_g}{2}\right)\ell}, \quad (\text{D6})$$

$$v_1 = v'_1 e^{(-C_0^A - C_0^B + C_1^A + C_1^B + C_g)\ell}, \quad (\text{D7})$$

$$v_2 = v'_2 e^{(-C_0^A - C_0^B + C_2^A + C_2^B + C_g)\ell}, \quad (\text{D8})$$

the action of fermions can be written as

$$S_{\Psi'} = \sum_{\sigma=1}^N \int \frac{d\omega'}{2\pi} \frac{d^2\mathbf{k}'}{(2\pi)^2} \bar{\Psi}'_\sigma(\omega', \mathbf{k}') [-i\omega'\gamma_0 + v'_1 k'_1 \gamma_1 + v'_2 k'_2 \gamma_2] \Psi'_\sigma(\omega', \mathbf{k}'), \quad (\text{D9})$$

which recovers the form of the original action.

The action for fermion-disorder coupling can be written as

$$S_{dis} = \sum_{\sigma=1}^N \int \frac{d\omega}{2\pi} \frac{d^2\mathbf{k}}{(2\pi)^2} \int \frac{d^2\mathbf{k}_1}{(2\pi)^2} \bar{\Psi}_\sigma(\omega, \mathbf{k}) v_\Gamma \Gamma \Psi_\sigma(\omega, \mathbf{k}_1) A(\mathbf{k} - \mathbf{k}_1) \quad (\text{D10})$$

Considering the corrections resulting from quantum fluctuation of EI order parameter, long-range Coulomb interaction, and disorder scattering, the action is given by

$$S_{dis} = \sum_{\sigma=1}^N \int \frac{d\omega}{2\pi} \frac{d^2\mathbf{k}}{(2\pi)^2} \int \frac{d^2\mathbf{k}_1}{(2\pi)^2} \bar{\Psi}_\sigma(\omega, \mathbf{k}) (v_\Gamma \Gamma + V^A + V^B + V_{dis}) \Psi_\sigma(\omega, \mathbf{k}_1) A(\mathbf{k} - \mathbf{k}_1). \quad (\text{D11})$$

Concretely, for RSP, we obtain

$$\begin{aligned} S_{dis} &= \sum_{\sigma=1}^N \int \frac{d\omega}{2\pi} \frac{d^2\mathbf{k}}{(2\pi)^2} \int \frac{d^2\mathbf{k}_1}{(2\pi)^2} \bar{\Psi}_\sigma(\omega, \mathbf{k}) [v_\Gamma \gamma_0 + v_\Gamma \gamma_0 (-C_0^A)\ell + v_\Gamma \gamma_0 (-C_0^B)\ell + v_\Gamma \gamma_0 C_g \ell] \Psi_\sigma(\omega, \mathbf{k}_1) A(\mathbf{k} - \mathbf{k}_1) \\ &\approx \sum_{\sigma=1}^N \int \frac{d\omega}{2\pi} \frac{d^2\mathbf{k}}{(2\pi)^2} \int \frac{d^2\mathbf{k}_1}{(2\pi)^2} \bar{\Psi}_\sigma(\omega, \mathbf{k}) v_\Gamma \gamma_0 e^{(-C_0^A - C_0^B + C_g)\ell} \Psi_\sigma(\omega, \mathbf{k}_1) A(\mathbf{k} - \mathbf{k}_1). \end{aligned} \quad (\text{D12})$$

For the two components of RVP, S_{dis} can be written as

$$\begin{aligned} S_{dis} &= \sum_{\sigma=1}^N \int \frac{d\omega}{2\pi} \frac{d^2\mathbf{k}}{(2\pi)^2} \int \frac{d^2\mathbf{k}_1}{(2\pi)^2} \bar{\Psi}_\sigma(\omega, \mathbf{k}) [v_\Gamma \gamma_1 + v_\Gamma \gamma_1 (-C_1^A)\ell + v_\Gamma \gamma_1 (-C_1^B)\ell] \Psi_\sigma(\omega, \mathbf{k}_1) A(\mathbf{k} - \mathbf{k}_1) \\ &\approx \sum_{\sigma=1}^N \int \frac{d\omega}{2\pi} \frac{d^2\mathbf{k}}{(2\pi)^2} \int \frac{d^2\mathbf{k}_1}{(2\pi)^2} \bar{\Psi}_\sigma(\omega, \mathbf{k}) v_\Gamma \gamma_1 e^{-(C_1^A + C_1^B)\ell} \Psi_\sigma(\omega, \mathbf{k}_1) A(\mathbf{k} - \mathbf{k}_1), \end{aligned} \quad (\text{D13})$$

and

$$\begin{aligned}
S_{\text{dis}} &= \sum_{\sigma=1}^N \int \frac{d\omega}{2\pi} \frac{d^2\mathbf{k}}{(2\pi)^2} \int \frac{d^2\mathbf{k}_1}{(2\pi)^2} \bar{\Psi}_\sigma(\omega, \mathbf{k}) [v_\Gamma \gamma_2 + v_\Gamma \gamma_2 (-C_2^A) \ell + v_\Gamma \gamma_2 (-C_2^B) \ell] \Psi_\sigma(\omega, \mathbf{k}_1) A(\mathbf{k} - \mathbf{k}_1) \\
&\approx \sum_{\sigma=1}^N \int \frac{d\omega}{2\pi} \frac{d^2\mathbf{k}}{(2\pi)^2} \int \frac{d^2\mathbf{k}_1}{(2\pi)^2} \bar{\Psi}_\sigma(\omega, \mathbf{k}) v_\Gamma \gamma_2 e^{-(C_2^A + C_2^B)\ell} \Psi_\sigma(\omega, \mathbf{k}_1) A(\mathbf{k} - \mathbf{k}_1),
\end{aligned} \tag{D14}$$

respectively. For RM, S_{dis} has the form

$$\begin{aligned}
S_{\text{dis}} &= \sum_{\sigma=1}^N \int \frac{d\omega}{2\pi} \frac{d^2\mathbf{k}}{(2\pi)^2} \int \frac{d^2\mathbf{k}_1}{(2\pi)^2} \bar{\Psi}_\sigma(\omega, \mathbf{k}) [v_\Gamma \mathbb{1} + v_\Gamma \mathbb{1} (C_0^A + C_1^A + C_2^A) \ell + v_\Gamma \mathbb{1} (C_0^B - C_1^B - C_2^B) \ell - v_\Gamma \mathbb{1} C_g \ell] \\
&\quad \times \Psi_\sigma(\omega, \mathbf{k}_1) A(\mathbf{k} - \mathbf{k}_1) \\
&= \sum_{\sigma=1}^N \int \frac{d\omega}{2\pi} \frac{d^2\mathbf{k}}{(2\pi)^2} \int \frac{d^2\mathbf{k}_1}{(2\pi)^2} \bar{\Psi}_\sigma(\omega, \mathbf{k}) v_\Gamma \mathbb{1} e^{(C_0^A + C_1^A + C_2^A + C_0^B - C_1^B - C_2^B - C_g)\ell} \Psi_\sigma(\omega, \mathbf{k}_1) A(\mathbf{k} - \mathbf{k}_1).
\end{aligned} \tag{D15}$$

Employing the re-scalings including Eqs. (D3)-(D6), and

$$A(\mathbf{k}) = A'(\mathbf{k}') e^\ell, \tag{D16}$$

and utilizing

$$v_\Gamma = v'_\Gamma \tag{D17}$$

for Eq. (D12),

$$v_\Gamma = v'_\Gamma e^{(-C_0^A - C_0^B + C_1^A + C_1^B + C_g)\ell} \tag{D18}$$

for Eq. (D13),

$$v_\Gamma = v'_\Gamma e^{(-C_0^A - C_0^B + C_2^A + C_2^B + C_g)\ell} \tag{D19}$$

for Eq. (D14),

$$v_\Gamma = v'_\Gamma e^{(-2C_0^A - C_1^A - C_2^A - 2C_0^B + C_1^B + C_2^B + 2C_g)\ell} \tag{D20}$$

for Eq. (D15), the action for the fermion-disorder coupling can be further written as

$$S_{\text{dis}} = \sum_{\sigma=1}^N \int \frac{d\omega'}{2\pi} \frac{d^2\mathbf{k}'}{(2\pi)^2} \int \frac{d^2\mathbf{k}'_1}{(2\pi)^2} \bar{\Psi}'_\sigma(\omega', \mathbf{k}') v'_\Gamma \mathbb{1} \Psi'_\sigma(\omega', \mathbf{k}'_1) A'(\mathbf{k}' - \mathbf{k}'_1), \tag{D21}$$

which restores the form of the original action.

From Eqs. (D6), we obtain the RG equation for the quasiparticle Z_f as following

$$\frac{dZ_f}{d\ell} = (C_0^A + C_0^B - C_g) Z_f. \tag{D22}$$

According to Eqs. (D7) and (D8), the RG equations for v_1 and v_2 can be written as

$$\frac{dv_1}{d\ell} = (C_0^A + C_0^B - C_1^A - C_1^B - C_g) v_1, \tag{D23}$$

$$\frac{dv_2}{d\ell} = (C_0^A + C_0^B - C_2^A - C_2^B - C_g) v_2. \tag{D24}$$

The RG equation for v_2/v_1 is given by

$$\begin{aligned}
\frac{d(v_2/v_1)}{d\ell} &= \frac{\frac{dv_2}{d\ell} v_1 - v_2 \frac{dv_1}{d\ell}}{v_1^2} \\
&= (C_1^A - C_2^A + C_1^B - C_2^B) \frac{v_2}{v_1}.
\end{aligned} \tag{D25}$$

Based on Eqs. (D17)-(D20), we obtain the RG equation for the parameter v_Γ

$$\left\{ \begin{array}{ll} \frac{dv_\Gamma}{d\ell} = 0, & \text{RSP,} \\ \frac{dv_\Gamma}{d\ell} = (C_0^A + C_0^B - C_1^A - C_1^B - C_g) v_\Gamma, & \gamma_1 \text{ component of RVP,} \\ \frac{dv_\Gamma}{d\ell} = (C_0^A + C_0^B - C_2^A - C_2^B - C_g) v_\Gamma, & \gamma_2 \text{ component of RVP,} \\ \frac{dv_\Gamma}{d\ell} = (2C_0^A + C_1^A + C_2^A + 2C_0^B - C_1^B - C_2^B - 2C_g) v_\Gamma, & \text{RM.} \end{array} \right. \quad (\text{D26})$$

-
- * Corresponding author: gzliu@ustc.edu.cn
- ¹ V. N. Kotov, B. Uchoa, V. M. Pereira, F. Guinea, and A. H. Castro Neto, *Rev. Mod. Phys.* **84**, 1067 (2012).
 - ² O. Vafek and A. Vishwanath, *Annu. Rev. Condens. Matter Phys.* **5**, 83 (2014).
 - ³ T. O. Wehling, A. M. Black-Schaffer, and A. V. Balatsky, *Adv. Phys.* **63**, 1 (2014).
 - ⁴ X. Wan, A. M. Turner, A. Vishwanath, and S. Y. Savrasov, *Phys. Rev. B* **83**, 205101 (2011).
 - ⁵ H. Weng, X. Dai, and Z. Fang, *J. Phys.: Condens. Matter* **28**, 303001 (2016).
 - ⁶ C. Fang, H. Weng, X. Dai, and Z. Fang, *Chin. Phys. B* **25**, 117106 (2016).
 - ⁷ B. Yan and C. Felser, *Annu. Rev. Condens. Matter Phys.* **8**, 337 (2017).
 - ⁸ M. Z. Hasan, S.-Y. Xu, I. Belopolski, and S.-M. Huang, *Annu. Rev. Condens. Matter Phys.* **8**, 289 (2017).
 - ⁹ N. P. Armitage, E. J. Mele, and A. Vishwanath, *Rev. Mod. Phys.* **90**, 015001 (2018).
 - ¹⁰ J. González, F. Guinea, and M. A. H. Vozmediano, *Phys. Rev. B* **59**, R2474(R) (1999).
 - ¹¹ J. Hofmann, E. Barnes, and S. Das Sarma, *Phys. Rev. Lett.* **113**, 105502 (2014).
 - ¹² A. Sharma and P. Kopietz, *Phys. Rev. B* **93**, 235425 (2016).
 - ¹³ P. Goswami and S. Chakravarty, *Phys. Rev. Lett.* **107**, 196803 (2011).
 - ¹⁴ P. Hosur, S. A. Parameswaran, and A. Vishwanath, *Phys. Rev. Lett.* **108**, 046602 (2012).
 - ¹⁵ J. Hofmann, E. Barnes, and S. Das Sarma, *Phys. Rev. B* **92**, 045104 (2015).
 - ¹⁶ R. E. Throckmorton, J. Hofmann, E. Barnes, and S. Das Sarma, *Phys. Rev. B* **92**, 115101 (2015).
 - ¹⁷ A. Sharma, A. Scammell, J. Krieg, and P. Kopietz, *Phys. Rev. B* **97**, 125113 (2018).
 - ¹⁸ B.-J. Yang, E.-G. Moon, H. Isobe, and N. Nagaosa, *Nat. Phys.* **10**, 774 (2014).
 - ¹⁹ A. A. Abrikosov, *J. Low. Temp. Phys.* **8**, 315 (1972).
 - ²⁰ A. A. Abrikosov and S. D. Beneslavskii, *Sov. Phys. JETP* **32**, 699 (1971).
 - ²¹ A. A. Abrikosov, *Sov. Phys. JETP* **39**, 709 (1974).
 - ²² E.-G. Moon, C. Xu, Y. B. Kim, and L. Balents, *Phys. Rev. Lett.* **111**, 206401 (2013).
 - ²³ I. F. Herbut and L. Janssen, *Phys. Rev. Lett.* **113**, 106401 (2014).
 - ²⁴ L. Janssen and I. F. Herbut, *Phys. Rev. B* **92**, 045117 (2015).
 - ²⁵ P. T. Dumitrescu, *Phys. Rev. B* **92**, 121102(R) (2015).
 - ²⁶ L. Janssen and I. F. Herbut, *Phys. Rev. B* **95**, 075101 (2017).
 - ²⁷ Y. Huh, E.-G. Moon, and Y. B. Kim, *Phys. Rev. B* **93**, 035138 (2016).
 - ²⁸ G. Y. Cho and E.-G. Moon, *Sci. Rep.* **6**, 19198 (2016).
 - ²⁹ H. Isobe and L. Fu, *Phys. Rev. B* **93**, 241113 (2016).
 - ³⁰ H.-H. Lai, *Phys. Rev. B* **91**, 235131 (2015).
 - ³¹ S.-K. Jian and H. Yao, *Phys. Rev. B* **92**, 045121 (2015).
 - ³² S.-X. Zhang, S.-K. Jian, and H. Yao, *Phys. Rev. B* **96**, 241111 (2017).
 - ³³ J.-R. Wang, G.-Z. Liu, and C.-J. Zhang, *Phys. Rev. B* **96**, 165142 (2017).
 - ³⁴ R. Shankar, *Rev. Mod. Phys.* **66**, 129 (1994).
 - ³⁵ A. H. Castro Neto, *Physics* **2**, 30 (2009).
 - ³⁶ D. V. Khveshchenko, *Phys. Rev. Lett.* **87**, 246802 (2001).
 - ³⁷ E. V. Gorbar, V. P. Gusynin, V. A. Miransky, and I. A. Shovkovy, *Phys. Rev. B* **66**, 045108 (2002).
 - ³⁸ D. V. Khveshchenko and H. Leal, *Nucl. Phys. B* **687**, 323 (2004).
 - ³⁹ G.-Z. Liu, W. Li, and G. Cheng, *Phys. Rev. B* **79**, 205429 (2009).
 - ⁴⁰ D. V. Khveshchenko, *J. Phys.:Condens. Matter* **21**, 075303 (2009).
 - ⁴¹ O. V. Gamayun, E. V. Gorbar, and V. P. Gusynin, *Phys. Rev. B* **81**, 075429 (2010).
 - ⁴² J. Sabio, F. Sols, and F. Guinea, *Phys. Rev. B* **82**, 121413(R) (2010).
 - ⁴³ C.-X. Zhang, G.-Z. Liu, and M.-Q. Huang, *Phys. Rev. B* **83**, 115438 (2011).
 - ⁴⁴ G.-Z. Liu and J.-R. Wang, *New J. Phys.* **13**, 033022 (2011).
 - ⁴⁵ J.-R. Wang and G.-Z. Liu, *J. Phys. Condens. Matter* **23**, 155602 (2011).
 - ⁴⁶ J.-R. Wang and G.-Z. Liu, *J. Phys. Condens. Matter* **23**, 345601 (2011).
 - ⁴⁷ J.-R. Wang and G.-Z. Liu, *New J. Phys.* **14**, 043036 (2012).
 - ⁴⁸ C. Popovici, C. S. Fischer, and L. von Smekal, *Phys. Rev. B* **88**, 205429 (2013).
 - ⁴⁹ J.-R. Wang and G.-Z. Liu, *Phys. Rev. B* **89**, 195404 (2014).
 - ⁵⁰ J. González, *Phys. Rev. B* **92**, 125115 (2015).
 - ⁵¹ M. E. Carrington, C. S. Fischer, L. von Smekal, and M. H. Thoma, *Phys. Rev. B* **94**, 125102 (2016).
 - ⁵² A. Sharma, V. N. Kotov, and A. H. Castro Neto, *Phys. Rev. B* **95**, 235124 (2017).
 - ⁵³ H.-X. Xiao, J.-R. Wang, H.-T. Feng, P.-L. Yin, and H.-S. Zong, *Phys. Rev. B* **96**, 155114 (2017).
 - ⁵⁴ M. E. Carrington, C. S. Fischer, L. von Smekal, and M. H.

- Thoma, Phys. Rev. B **97**, 115411 (2018).
- ⁵⁵ O. V. Gamayun, E. V. Gorbar, and V. P. Gusynin, Phys. Rev. B **80**, 165429 (2009).
- ⁵⁶ J. Wang, H. A. Fertig, G. Murthy, and L. Brey, Phys. Rev. B **83**, 035404 (2011).
- ⁵⁷ A. Katanin, Phys. Rev. B **93**, 035132 (2016).
- ⁵⁸ J. González, Phys. Rev. B **82**, 155404 (2010).
- ⁵⁹ J. González, Phys. Rev. B **85**, 085420 (2012).
- ⁶⁰ J. E. Drut and T. A. Lähde, Phys. Rev. Lett. **102**, 026802 (2009).
- ⁶¹ J. E. Drut and T. A. Lähde, Phys. Rev. B **79**, 165425 (2009).
- ⁶² J. E. Drut and T. A. Lähde, Phys. Rev. B **79**, 241405(R) (2009).
- ⁶³ W. Armour, S. Hands, and C. Strouthos, Phys. Rev. B **81**, 125105 (2010).
- ⁶⁴ W. Armour, S. Hands, and C. Strouthos, Phys. Rev. B **84**, 075123 (2011).
- ⁶⁵ P. V. Buividovich and M. I. Polikarpov, Phys. Rev. B **86**, 245117 (2012).
- ⁶⁶ F. de Juan and H. A. Fertig, Solid State Commun. **152**, 1460 (2012).
- ⁶⁷ M. V. Ulybyshev, P. V. Buividovich, M. I. Katsnelson, and M. I. Polikarpov, Phys. Rev. Lett. **111**, 056801 (2013).
- ⁶⁸ D. Smith and L. von Smekal, Phys. Rev. B **89**, 195429 (2014).
- ⁶⁹ A. V. Kotikov and S. Teber, Phys. Rev. D **94**, 114010 (2016).
- ⁷⁰ J. González, Phys. Rev. B **90**, 121107(R) (2014).
- ⁷¹ V. V. Braguta, M. I. Katsnelson, A. Y. Kotov, and A. A. Nikolaev, Phys. Rev. B **94**, 205147 (2016).
- ⁷² H.-X. Xiao, J.-R. Wang, G.-Z. Liu, and H.-S. Zong, Phys. Rev. B **97**, 155122 (2018).
- ⁷³ L. Janssen and I. F. Herbut, Phys. Rev. B **93**, 165109 (2016).
- ⁷⁴ J.-R. Wang, G.-Z. Liu, and C.-J. Zhang, Phys. Rev. B **95**, 075129 (2017).
- ⁷⁵ L. V. Keldysh and Y. V. Kopayev, Fiz. Tverd. Tela. **6**, 2791 (1964).
- ⁷⁶ D. Jerome, T. M. Rice, and W. Kohn, Phys. Rev. **158**, 462 (1967).
- ⁷⁷ Y. Nambu and G. Jona-Lasinio, Phys. Rev. **122**, 345 (1961).
- ⁷⁸ V. A. Miransky, *Dynamical Symmetry Breaking in Quantum Field Theories*, (World Scientific, 1994).
- ⁷⁹ D. C. Elias, R. V. Gorbachev, A. S. Mayorov, S. V. Morozov, A. A. Zhukov, P. Blake, L. A. Ponomarenko, I. V. Grigorieva, K. S. Novoselov, F. Guinea, and A. K. Geim, Nat. Phys. **7**, 701 (2011).
- ⁸⁰ H.-K. Tang, E. Laksono, J. N. B. Rodrigues, P. Sengupta, F. F. Assad, and S. Adam, Phys. Rev. Lett. **115**, 186602 (2015).
- ⁸¹ M. Hirata, K. Ishikawa, G. Matsuno, A. Kobayashi, K. Miyagawa, M. Tamura, C. Berthier, and K. Kanoda, Science **358**, 1403 (2017).
- ⁸² C. Triola, E. Rossi, and A. V. Balatsky, Phys. Rev. B **89**, 165309 (2014).
- ⁸³ Y. Huh and S. Sachdev, Phys. Rev. B **78**, 064512 (2008).
- ⁸⁴ J.-R. Wang, G.-Z. Liu, and C.-J. Zhang, New J. Phys. **18**, 073023 (2016).
- ⁸⁵ D. A. Siegel, C.-H. Park, C. Hwang, J. Deslippe, A. V. Fedorov, S. G. Louie, and A. Lanzara, Proc. Natl. Acad. Sci. U.S.A. **108**, 11365 (2011).
- ⁸⁶ J. Chae, S. Jung, A. F. Young, C. R. Dean, L. Wang, Y. Gao, K. Watanabe, T. Taniguchi, J. Hone, K. L. Shepard, P. Kim, N. B. Zhitenev, and J. A. Stroscio, Phys. Rev. Lett. **109**, 116802 (2012).
- ⁸⁷ G. L. Yu, R. Jalil, B. Belle, A. S. Mayorov, P. Blake, F. Schedin, S. V. Morozov, L. A. Ponomarenko, F. Chiappini, S. Wiedmann, U. Zeitler, M. I. Katsnelson, A. K. Geim, K. S. Novoselov, and D. C. Elias, Proc. Natl. Acad. Sci. U.S.A. **110**, 3282 (2013).
- ⁸⁸ J. Ye and S. Sachdev, Phys. Rev. Lett. **80**, 5409 (1998).
- ⁸⁹ J. Ye, Phys. Rev. B **60**, 8290 (1999).
- ⁹⁰ T. Stauber, F. Guinea, and M. A. H. Vozmediano, Phys. Rev. B **71**, 041406(R) (2005).
- ⁹¹ I. F. Herbut, V. Juričić, and O. Vafek, Phys. Rev. Lett. **100**, 046403 (2008).
- ⁹² O. Vafek and M. J. Case, Phys. Rev. B **77**, 033410 (2008).
- ⁹³ M. S. Foster and I. L. Aleiner, Phys. Rev. B **77**, 195413 (2008).